Standard model with four generations: Selected implications for rare B and K decays

Amarjit Soni,[1] Ashutosh Kumar Alok,[2] Anjan Giri,[3] Rukmani Mohanta,[4] and Soumitra Nandi[5]

[1]*Physics Department, Brookhaven National Laboratory, Upton, New York 11973, USA*

[2]*Physique des Particules, Université de Montréal, Case Postale 6128, Succursale centre-ville, Montréal, Quebec, Canada H3C 3J7*

[3]*Physics Department, IIT Hyderabad, Andhra Pradesh-502205, India*

[4]*School of Physics, University of Hyderabad, Hyderabad - 500046, India*

[5]*Dipartimento di Fisica Teorica, Universita di Torino and INFN, Sezione di Torino, I-10125 Torino, Italy*

(Received 19 May 2010; published 13 August 2010)

We extend our recent work and study implications of the standard model with four generations (SM4) for rare B and K decays. We again take seriously the several 2–3σ anomalies seen in B, B_s decays and interpret them in the context of this simple extension of the SM. SM4 is also of course of considerable interest for its potential relevance to dynamical electroweak symmetry breaking and to baryogenesis. Using experimental information from processes such as $B \to X_s \gamma$, B_d and B_s mixings, indirect CP-violation from $K_L \to \pi\pi$ etc. along with oblique corrections, we constrain the relevant parameter space of the SM4, and find $m_{t'}$ of about 400–600 GeV with a mixing angle $|V^*_{t'b} V_{t's}|$ in the range of about 0.05–1.4×10^{-2} and with an appreciable CP-odd associated phase, are favored by the current data. Given the unique role of the CP asymmetry in $B_s \to \psi\phi$ due to its gold-plated nature, correlation of that with many other interesting observables, including the semileptonic asymmetry ($A_{\rm SL}$) are studied in SM4. We also identify several processes, such as $B \to X_s \nu\bar{\nu}$, $K_L \to \pi^0 \nu\bar{\nu}$ etc., that are significantly different in SM4 from the SM. Experimentally the very distinctive process $B_s \to \mu^+\mu^-$ is also discussed; the branching ratio can be larger or smaller than in SM, $(3.2 \to 4.2) \times 10^{-9}$, by a factor of $\mathcal{O}(3)$.

DOI: 10.1103/PhysRevD.82.033009 PACS numbers: 14.40.Nd, 13.20.Eb, 14.65.Jk

I. INTRODUCTION

Though the Cabibbo-Kobayashi-Maskawa (CKM) paradigm [1,2] of CP violation in the standard model (SM) has been extremely successful in describing a multitude of experimental data, in the past few years some indications of deviations have surfaced, specifically in the flavor sector [3–7]. An intriguing aspect of these deviations is that so far they have more prominently, though not exclusively, occurred in CP violating observables only. While many beyond the standard model (BSM) scenarios can account for such effects [8–14], a very simple extension of the SM that can cause these anomalies is the addition of an extra family as we emphasized in a recent study [15,16]. In this paper, we will extend our previous work and study the implications of the standard model with four generations (SM4) in rare B and K decays.

Although our initial motivation for studying SM4 was triggered by the deviations in the CP violating observables in B, B_s decays, we want to stress that actually SM4 is, in fact, a very simple and interesting extension of the three generation SM (SM3). The fact that the heavier quarks and leptons in this family can play a crucial role in dynamical electroweak-symmetry breaking (DEWSB) as an economical way to address the hierarchy puzzle renders this extension of SM3 especially interesting. In addition, whereas, as is widely recognized SM3 does not have enough CP to facilitate baryogenesis, that difficulty is readily and significantly ameliorated in SM4 [17–19]. Besides, given that three families exist, it is clearly important to search for the fourth.

That rare B-decays are particularly sensitive to the fourth generation was in fact emphasized long ago [20–24]. The potential role of heavy quarks in DEWSB was also another reason for the earlier interest [25–29]. LEP/SLC discovery that a fourth family (essentially) massless neutrino does not exist was one reason that caused some pause in the interest on SM4. A decade later discovery of neutrino oscillations and of neutrino mass managed to offset to some degree this concern about the 4th family's necessarily involving massive neutrino. Electroweak precision tests provide a very important constraint on the mass difference of the 4th family isodoublet. In this context the PDG reviewer's statement [30] that a degenerate 4th family is strongly disfavored by electroweak precision (EWP) tests may have been widely misinterpreted; careful studies show in fact that while mass difference between the isodoublet quarks is constrained to be less than ≈ 75 GeV, an extra generation of quarks is not excluded by the current data. In fact, some have also claimed that for certain values of particle masses the quality of the fit with four generations is comparable to that of the SM3 [31–34].[1]

The addition of fourth generation to the SM means that the quark mixing matrix will now become a 4×4 matrix ($V_{\rm CKM4}$) and the parametrization of this unitary matrix

[1]After this paper had been submitted for publication, very recently, authors of Ref. [30] have reported a new analysis wherein they state that while their reanalysis with the new data does not exclude the fourth generation, the fit is not as good as the SM; see Ref. [35]

requires six real parameters and three phases. The two extra phases imply the possibility of extra sources of CP violation [22].

In [15], it was shown that a fourth family of quarks with $m_{t'}$ in the range of (400–600) GeV provides a simple explanation for the several indications of new physics that have been observed involving CP asymmetries in the B, B_s decays [3–7]. The built-in hierarchy of $V_{\rm CKM4}$ is such that the t' readily provides a needed perturbation ($\approx 15\%$) to $\sin 2\beta$ as measured in $B \to \psi K_s$ and simultaneously is the dominant source of CP asymmetry in $B_s \to \psi\phi$.

While most of the B, B_s CP-anomalies are easily accommodated and explained by SM4, we note that, in contrast, EW precision tests constrain the mass-splitting between t' and b' to be small, around 70 GeV [31–33,36]; so for $m_{t'}$ of $O(500\ \text{GeV})$ their masses have to be degenerate to $O(15\%)$. As far as the lepton sector is concerned, it is clear that the 4th family lepton has to be quite different from the previous three families in that the neutral lepton has to be rather massive, with mass $> m_Z/2$. This may also be a clue that the underlying nature of the 4th family may be quite different from the previous three families [37]. At this stage we would like to mention that the addition of fourth generation will also change the lepton mixing matrix (PMNS) [38]. The new elements in the PMNS matrix could be constrained from lepton flavor violation in the charged and neutral sectors, for example, a more stringent constraint on first/second generation mixings with the fourth generation should come from $\mu \to e\gamma$. In a similar way one could constrain third/fourth generation mixings from $\tau \to \mu\gamma$ lepton flavor violating decay. However in this paper our primary focus is on the quark sector, so in order to avoid any detailed assumptions about the heavy lepton masses and their mixing with SM3 lepton generations, in our numerical analysis we will be neglecting the off-diagonal terms of the PMNS matrix.

In this paper we extend our previous work [15] on the implications of SM4, to study the direct CP asymmetry in $B \to X_s\gamma$, $B \to X_s l^+ l^-$ and in $B_s \to X_s \ell \nu$, forward-backward (FB) asymmetry in $B \to X_s(K^*) l^+ l^-$, decay rates of $B \to X_s \nu\bar{\nu}$, $B_s \to \mu^+\mu^-$, $\tau^+\tau^-$, and $K_L \to \pi^0 \nu\bar{\nu}$ and CP violation in $B \to \pi K$ and $B^0 \to \pi^0\pi^0$ modes. We show that SM4 can ameliorate the difficulty in understanding the large difference, $O(15\%)$, between the direct CP asymmetries in neutral B decays to $K^+\pi^-$ versus that of the charged B-decays to $K^+\pi^0$ partly due to the enhanced isospin violation that SM4 causes in flavor-changing penguin transitions due to the heavy $m_{t'}$ [20] originating from the evasion of the decoupling theorem and partly if the corresponding strong phase(s) are large in SM4. The enhanced electroweak penguin amplitude provides a color-allowed ($Z \to \pi^0$) contribution which is not present for $\pi^\pm$ case. However, we want to emphasize that the prediction obtained using the QCD factorization approach [3,39,40] depends on many input parameters therefore it has large theoretical uncertainties. Apart from the SM parameters such as CKM matrix, quark masses, the strong coupling constant and hadronic parameters there are large theoretical uncertainties related to the modeling of power corrections corresponding to weak annihilation effects and the chirally-enhanced power corrections to hard spectator scattering. Therefore the numerical results for the direct CP asymmetries are not reliable.

Several of these observables like FB asymmetry in $B \to K^* l^+ l^-$ [41], CP asymmetry in $B_s \to \psi\phi$ [42] and the decay rate of $K_L \to \pi^0\nu\bar{\nu}$ [43] have also been studied before, as well as many other interesting aspects of SM4 by Hou and collaborators [44–47], see also [48]. However, their analysis was generally restricted to $m_{t'}$ of $\sim$300 GeV. On the other hand, our analysis seems to favor $m_{t'}$ in the range of (400–600) GeV to explain the observed CP asymmetries in the B, B_s decays. We note also that recent analysis by Chanowitz seems to disfavor most of the parameter space they have used [34] whereas our parameter space is largely unaffected [49].

We identify several processes wherein SM4 causes large deviations from the expectations of SM3; for example, $B \to X_s \nu\bar{\nu}$, $B_s \to \mu^+\mu^-$, $A_{\rm SL}(B_s \to X_s \ell\nu)$, $a_{CP}(B \to \pi K)$, $a_{CP}(B \to \pi^0\pi^0)$, $K_L \to \pi^0\nu\bar{\nu}$ and of course mixing-induced CP in $B_s \to \psi\phi$, etc. These observables will be measured with higher statistics at the upcoming high intensity K, B, B_s experiments at CERN, FERMILAB, JPARC facilities, etc. and, in particular, at the LHCb experiment and possibly also at the Super-B factories and hence may provide further indirect evidence for an additional family of quarks.

The paper is arranged as follows. After the introduction, we provide constraints on the 4×4 CKM matrix by incorporating oblique corrections along with experimental data from important observables involving Z, B, and K decays as well as B_d and B_s mixings, etc. In Sec. III, we present the estimates of many useful observables in the SM4. Finally, in Sec. IV, we present our summary.

II. CONSTRAINTS ON THE CKM4 MATRIX ELEMENTS

In our previous article [15], to find the limits on $V_{\rm CKM4}$ elements, we concentrated mainly on the constraints that will come from vertex correction to $Z \to b\bar{b}$, $\text{Br}(B \to X_s\gamma)$, $\text{Br}(B \to X_s l^+ l^-)$, $B_d - \bar{B}_d$, and $B_s - \bar{B}_s$ mixing, $\text{Br}(K^+ \to \pi^+\nu\nu)$ and indirect CP violation in $K_L \to \pi\pi$ described by $|\epsilon_k|$. We did not consider ϵ'/ϵ as a constraint because of its large hadronic uncertainties. Chanowitz [34] has shown that as $m_{t'}$ becomes very large a more important constraint is from non–decoupling oblique corrections rather than the vertex correction to $Z \to b\bar{b}$. In this article we have extended our analysis by including the constraint from non–decoupling oblique corrections as well; we note that for $m_{t'} \lesssim 500$ GeV our previous constraints are largely unaffected but for $m_{t'} \approx 600$ GeV the oblique cor-

TABLE I. Inputs that we use in order to constrain the SM4 parameter space, we have considered the 2σ range for V_{ub}.

$B_K = 0.72 \pm 0.05$ [50]	$f_{bs}\sqrt{B_{bs}} = 0.281 \pm 0.021$ GeV [51]
$\Delta M_s = (17.77 \pm 0.12)\ \mathrm{ps}^{-1}$ [52]	$\Delta M_d = (0.507 \pm 0.005)\ \mathrm{ps}^{-1}$
$\xi_s = 1.2 \pm 0.06$ [51]	$\gamma = (75.0 \pm 22.0)^\circ$
$\vert\epsilon_k\vert \times 10^3 = 2.32 \pm 0.007$	$\sin 2\beta_{\psi K_s} = 0.672 \pm 0.024$
$\mathrm{Br}(K^+ \to \pi^+ \nu\nu) = (0.147^{+0.130}_{-0.089}) \times 10^{-9}$	$\mathrm{Br}(B \to X_c \ell \nu) = (10.61 \pm 0.17) \times 10^{-2}$
$\mathrm{Br}(B \to X_s \gamma) = (3.55 \pm 0.25) \times 10^{-4}$	$\mathrm{Br}(B \to X_s \ell^+ \ell^-) = (0.44 \pm 0.12) \times 10^{-6}$
$R_{bb} = 0.216 \pm 0.001$	(High q^2 region)
$\vert V_{ub}\vert = (37.2 \pm 2.7) \times 10^{-4}$	$\vert V_{cb}\vert = (40.8 \pm 0.6) \times 10^{-3}$
$\eta_c = 1.51 \pm 0.24$ [53]	$\eta_t = 0.5765 \pm 0.0065$ [54]
$\eta_{ct} = 0.47 \pm 0.04$ [55]	$m_t = 172.5$ GeV
$T_4 = 0.11 \pm 0.14$	

rections start to have effect. With the inputs given in Table I we have made the scan over the entire parameter space by a flat random number generator and obtained the constraints on various parameters of the 4×4 mixing matrix (Table II). In the following subsections we briefly discuss the various input parameters used in our analysis.

A. Oblique correction

The Z pole, W mass, and low-energy data can be used to search for and set limits on deviations from the SM. Most of the effects on precision measurements can be described by the three gauge self-energy parameters S, T, and U. We assume these parameters to be arising from new physics only, i.e. they are equal to zero exactly in SM, and do not include any contributions from m_t and M_H.

The effects of nondegenerate multiplets of chiral fermions can be described by just three parameters, S, T, and U at the one-loop level [30,31,56–58]. T is proportional to the difference between the W and Z self-energies at $Q^2 = 0$, while S is associated with the difference between the Z self-energy at $Q^2 = M_Z^2$ and $Q^2 = 0$ and $(S + U)$ is associated with the difference between W self-energy at $Q^2 = M_W^2$ and $Q^2 = 0$. A nondegenerate $SU(2)$ doublet

$$\begin{pmatrix} f1 \\ f2 \end{pmatrix}$$

with masses m_1 and m_2 respectively yields the contributions [56]

$$S = \frac{1}{6\pi}[1 - Y \ln(m_1^2/m_2^2)],$$
$$T = \frac{1}{16\pi s_W^2 c_W^2 M_Z^2}\left[m_1^2 + m_2^2 - \frac{2m_1^2 m_2^2}{m_1^2 - m_2^2}\ln(m_1^2/m_2^2)\right],$$
$$U = \frac{1}{6\pi}\left[-\frac{5m_1^4 - 22m_1^2 m_2^2 + 5m_2^4}{3(m_1^2 - m_2^2)^2} + \frac{m_1^6 - 3m_1^4 m_2^2 - 3m_1^2 m_2^4 + m_2^6}{(m_1^2 - m_2^2)^3}\ln(m_1^2/m_2^2)\right], \quad (1)$$

where Y is the hypercharge of the doublet. A heavy nondegenerate doublet of fermions contributes positively to T as

$$\rho_0^* - 1 = \frac{1}{1 - \alpha T} - 1 \approx \alpha T, \quad (2)$$

where ρ_0^* denotes the low-energy ratio of neutral to charged current couplings in neutrino interactions.

The parameter U plays a fairly unimportant role, all the neutral current and low energy observables depend only on S and T [56]. In addition U is often predicted to be very small. In most of the models U should differ from zero by only a percent of T.

Contributions to T and S parameters from fourth family quarks and leptons, with doublets

$$\begin{pmatrix} t' \\ b' \end{pmatrix}$$

and

$$\begin{pmatrix} \ell_4 \\ \nu_4 \end{pmatrix}$$

respectively, are given by [34]

$$T_4 = \frac{1}{8\pi x_W(1 - x_W)}[3(|V_{t'b'}|^2 \delta m_{t'b'} + |V_{t'b}|^2 \delta m_{t'b} + |V_{tb'}|^2 \delta m_{tb'} - |V_{t'b}|^2 \delta m_{tb} + |V_{t's}|^2 \delta m_{t's}) + \delta m_{\ell_4 \nu_4}], \quad (3)$$

TABLE II. Allowed ranges for the parameters, $\lambda^s_{t'}$ ($\times 10^{-2}$) and phase ϕ'_s (in degree) for different masses $m_{t'}$ (GeV), that have been obtained from the fitting with the inputs in Table I and allowed by the present experimental bound for CP asymmetry in $B_s \to J/\psi\phi$ [15].

$m_{t'}$ (GeV)	300	400	500	600
$\lambda^s_{t'}$	(0.09–2.5)	(0.08–1.4)	(0.06–0.9)	(0.05–0.6)
ϕ'_s	$0 \to 80$	$0 \to 80$	$0 \to 80$	$0 \to 80$

$$S_4 = \frac{N_c}{6\pi}\left(1 - \frac{1}{3}\ln\frac{m_{t'}^2}{m_{b'}^2} + \ln\frac{m_{\ell_4}^2}{m_{\nu_4}^2}\right), \tag{4}$$

with

$$\delta m_{12} = \frac{1}{2M_Z^2}\left(m_1^2 + m_2^2 - \frac{2m_1^2 m_2^2}{m_1^2 - m_2^2}\ln(m_1^2/m_2^2)\right). \tag{5}$$

Here $N_c = 3$ for a quark family and the same formula with $N_c = 1$ will be for a 4th generation lepton family.

B. Vertex corrections to $Z \to b\bar{b}$

Including QCD and QED corrections, the $Z \to b\bar{b}$ decay width can be written as [59]

$$\Gamma(Z \to q\bar{q}) = \frac{N_c}{48}\frac{\alpha}{s_W^2 c_W^2} m_Z(|a_q|^2 + |v_q|^2) \times (1 + \delta_b^{(0)})(1 + \delta_{\mathrm{QED}}^q)(1 + \delta_{\mathrm{QCD}}^q)(1 + \delta_\mu^q) \times (1 + \delta_{t\mathrm{QCD}}^q)(1 + \delta_q), \tag{6}$$

where

$$v_q = (2I_3^q - 4|Q_q|s_W^2), \qquad a_q = 2I_3^q, \tag{7}$$

and δ's are various corrections which are discussed below.

In the decay of the $Z \to b\bar{b}$, the top quark mass enters in the loop correction to the vertex mediated by the W gauge boson. Because of spontaneous symmetry breaking effects the top mass cannot be neglected in the calculation. In fact, there is a top mass dependence that grows like $\frac{m_t^2}{m_Z^2}$ as in many other one-loop weak processes such as $K - \bar{K}$, $B - \bar{B}$ ($\Delta F = 2$ mixings), $b \to s\ell^+\ell^-$, etc. The additional contribution to the $Zb\bar{b}$ vertex, due to nonzero value of the top quark mass can be written as

$$\delta_b \approx 10^{-2}\left(\left(-\frac{m_t^2}{2m_Z^2} + 0.5\right)|V_{tb}|^2 + \left(-\frac{m_{t'}^2}{2m_Z^2} + 0.5\right)|V_{t'b}|^2\right). \tag{8}$$

δ_{QED}^q gives small final-state QED corrections that depend on the charge of final fermion,

$$\delta_{\mathrm{QED}}^q = \frac{3\alpha}{4\pi}Q_q^2. \tag{9}$$

It is very small (0.2% for charged leptons, 0.8% for u-type quarks and 0.02% for d-type quarks).

δ_{QCD} gives the QCD corrections common to all quarks and it is given by

$$\delta_{\mathrm{QCD}} = \frac{\alpha_s}{\pi} + 1.41\left(\frac{\alpha_s}{\pi}\right)^2. \tag{10}$$

α_s is the QCD coupling constant taken at the m_Z scale, i.e. $\alpha_s = \alpha_s(m_Z^2) = 0.12$.

δ_μ^q contains the kinematical effects of the external fermion masses, including some mass-dependent QCD radiative corrections. It is only important for the b-quark (0.5%) and to a lesser extent for the τ-lepton (0.2%) and the c-quark (0.05%). It is given by

$$\delta_\mu^q = \frac{3\mu_q^2}{v_q^2 + a_q^2}\left(-\frac{1}{2}a_q^2\left(1 + \frac{8\alpha_s}{3\pi}\right) + v_q^2\frac{\alpha_s}{\pi}\right), \tag{11}$$

where $\mu_q^2 \equiv 4\bar{m}_q^2(m_Z^2)/m_Z^2$.

By taking appropriate branching ratios it is possible to isolate the large top mass dependent $Zb\bar{b}$ vertex δ_b [59],

$$R_h \equiv \frac{\Gamma(Z \to b\bar{b})}{\Gamma(Z \to \mathrm{hadrons})} = (1 + 2/R_s + 1/R_c + 1/R_u)^{-1}, \tag{12}$$

where $R_q \equiv \frac{\Gamma(Z \to b\bar{b})}{\Gamma(Z \to q\bar{q})}$.

All other corrections cancel exactly in this branching ratio except the correction to the $Zb\bar{b}$ vertex which only depends on the top quark mass.

C. $B \to X_s\gamma$ decay

Radiative B decays have been a topic of great theoretical and experimental interest for long. Although the inclusive radiative decay $B \to X_s\gamma$ is loop suppressed within the SM, it has a relatively large branching ratio making it statistically favorable from the experimental point of view and hence it serves as an important probe to test SM and its possible extensions. The present world average of $\mathrm{Br}(B \to X_s\gamma)$ is $(3.55 \pm 0.25) \times 10^{-4}$ [60], which is in good agreement with its SM prediction [61,62]. Apart from the branching ratio of $B \to X_s\gamma$, direct CP violation in $B \to X_s\gamma$, $A_{CP}^{B\to X_s\gamma}$ can serve as an important observable to search physics beyond SM; therefore we will also study this direct CP asymmetry in this paper (see Sec. III A).

The quark level transition $b \to s\gamma$ induces the inclusive $B \to X_s\gamma$ decay. The effective Hamiltonian for $b \to s\gamma$ can be written in the following form

$$\mathcal{H}_{\mathrm{eff}} = \frac{4G_F}{\sqrt{2}}V_{ts}^* V_{tb}\sum_{i=1}^{8} C_i(\mu)Q_i(\mu), \tag{13}$$

where the form of operators $O_i(\mu)$ and the expressions for calculating the Wilson coefficients $C_i(\mu)$ are given in [63]. The introduction of fourth generation changes the values of Wilson coefficients C_7 and C_8 via the virtual exchange of the t'-quark and can be written as

$$C_{7,8}^{\mathrm{tot}}(\mu) = C_{7,8}(\mu) + \frac{V_{t's}^* V_{t'b}}{V_{ts}^* V_{tb}}C_{7,8}^{t'}(\mu). \tag{14}$$

The values of $C_{7,8}^{t'}$ can be calculated from the expression of $C_{7,8}$ by replacing the mass of t-quark by $m_{t'}$.

In order to reduce the uncertainties arising from b-quark mass, we consider the following ratio

$$R = \frac{\mathrm{Br}(B \to X_s \gamma)}{\mathrm{Br}(B \to X_c e \bar{\nu}_e)}.$$

In leading logarithmic approximation this ratio can be written as [64]

$$R = \frac{|V_{ts}^* V_{tb}|^2}{|V_{cb}|^2} \frac{6\alpha |C_7^{\mathrm{tot}}(m_b)|^2}{\pi f(\hat{m}_c)\kappa(\hat{m}_c)}. \tag{15}$$

Here the Wilson coefficient C_7 is evaluated at the scale $\mu = m_b$. The phase space factor $f(\hat{m}_c)$ in $\mathrm{Br}(B \to X_c e \bar{\nu})$ is given by [65]

$$f(\hat{m}_c) = 1 - 8\hat{m}_c^2 + 8\hat{m}_c^6 - \hat{m}_c^8 - 24\hat{m}_c^4 \ln \hat{m}_c. \tag{16}$$

$\kappa(\hat{m}_c)$ is the 1-loop QCD correction factor [65]

$$\kappa(\hat{m}_c) = 1 - \frac{2\alpha_s(m_b)}{3\pi}\left[\left(\pi^2 - \frac{31}{4}\right)(1 - \hat{m}_c)^2 + \frac{3}{2}\right]. \tag{17}$$

Here $\hat{m}_c = m_c/m_b$.

D. $B \to X_s l^+ l^-$ decay

The quark level transition $b \to s l^+ l^-$ is responsible for the inclusive decay $B \to X_s l^+ l^-$. We apply the same approach introduced for $b \to s\gamma$. The effective Hamiltonian for the decay $b \to s l^+ l^-$ is given by

$$\mathcal{H}_{\mathrm{eff}} = \frac{4G_F}{\sqrt{2}} V_{ts}^* V_{tb} \sum_{i=1}^{10} C_i(\mu) Q_i(\mu). \tag{18}$$

In addition to the operators relevant for $b \to s\gamma$, there are two new operators:

$$Q_9 = (\bar{s}b)_{V-A}(\bar{l}l)_V, \qquad Q_{10} = (\bar{s}b)_{V-A}(\bar{l}l)_V. \tag{19}$$

The amplitude for the decay $B \to X_s l^+ l^-$ in SM4 is given by

$$M = \frac{G_F \alpha}{\sqrt{2}\pi} V_{ts}^* V_{tb}\bigg[C_9^{\mathrm{tot}} \bar{s}\gamma_\mu P_L b \bar{l}\gamma_\mu l + C_{10}^{\mathrm{tot}} \bar{s}\gamma_\mu P_L b \bar{l}\gamma_\mu \gamma_5 l - 2m_b \frac{C_7^{\mathrm{tot}}}{q^2} \bar{s} i\sigma_{\mu\nu} q^\nu P_R b \bar{l}\gamma_\mu l\bigg], \tag{20}$$

where $P_{L,R} = (1 \mp \gamma_5)/2$ and q is the sum of l^+ and l^- momenta. Here the Wilson coefficients are evaluated at $\mu = m_b$.

The differential branching ratio is given by

$$\frac{d\,\mathrm{Br}(B \to X_s l^+ l^-)}{dz} = \frac{\alpha^2 B(B \to X_c e \bar{\nu})}{4\pi^2 f(\hat{m}_c)\kappa(\hat{m}_c)}(1-z)^2 \times \left(1 - \frac{4t^2}{z}\right)^{1/2} \frac{|V_{tb}^* V_{ts}|^2}{|V_{cb}|^2} D(z), \tag{21}$$

where

$$D(z) = |C_9^{\mathrm{tot}}|^2\left(1 + \frac{2t^2}{z}\right)(1+2z) + 4|C_7^{\mathrm{tot}}|^2\left(1 + \frac{2t^2}{z}\right) \times \left(1 + \frac{2}{z}\right) + |C_{10}^{\mathrm{tot}}|^2\left[(1+2z) + \frac{2t^2}{z}(1-4z)\right] + 12\,\mathrm{Re}(C_7^{\mathrm{tot}} C_9^{\mathrm{tot}*})\left(1 + \frac{2t^2}{z}\right). \tag{22}$$

Here $z \equiv q^2/m_b^2$, $t \equiv m_l/m_b$, and $\hat{m}_q = m_q/m_b$ for all quarks q.

In the framework of SM4, the Wilson coefficients C_7^{tot}, C_9^{tot}, and C_{10}^{tot} are given by

$$C_{7,10}^{\mathrm{tot}} = C_{7,10}(m_b) + \frac{V_{t's}^* V_{t'b}}{V_{ts}^* V_{tb}} C_{7,10}^{t'}(m_b), \tag{23}$$

$$C_9^{\mathrm{tot}} = C_9(m_b) + Y(z) + \frac{V_{t's}^* V_{t'b}}{V_{ts}^* V_{tb}} C_9^{t'}(m_b), \tag{24}$$

where the function $Y(z)$ is given in [63].

The measurements of the $B \to X_s \ell^+ \ell^-$ in the two regions, so-called low q^2 ($q^2 \lesssim 6\ \mathrm{GeV}^2$) and high q^2 ($q^2 \gtrsim 14\ \mathrm{GeV}^2$), are complementary as they have different sensitivities to the short distance physics. Compared to small q^2, the rate in the large q^2 region has a smaller renormalization scale dependence and m_c dependence. Although the rate is smaller at large q^2, the experimental efficiency is better. Large q^2 constrains the X_s to have small invariant mass, m_{X_s}, which suppresses the background from $B \to X_c \ell^- \bar{\nu} \to X_s \ell^+ \ell^- \nu \bar{\nu}$. To suppress this background at small q^2 region an upper cut on m_{X_s} is required, complicating the theoretical description due to the dependence of the measured rate on the shape function, which is absent at large q^2. In the low q^2 region the dominant contribution to $B_s \to X_s \ell^+ \ell^-$ comes from virtual photon and much less from Z. It is the Z that is very sensitive to $m_{t'}$ as that amplitude grow with $m_{t'}^2$. The photonic contribution cares only about the electric charge, modulo logarithmic QCD corrections. For these reasons we will be using the branching ratio only in the high q^2 region to constrain SM4.

The theoretical calculations shown above for the branching ratio of $B \to X_s l^+ l^-$ are rather uncertain in the intermediate q^2 region ($7\ \mathrm{GeV}^2 < q^2 < 12\ \mathrm{GeV}^2$) owing to the vicinity of charmed resonances. The predictions are relatively more robust in the low-q^2 ($1\ \mathrm{GeV}^2 < q^2 < 6\ \mathrm{GeV}^2$) and the high-$q^2$ ($14.4\ \mathrm{GeV}^2 < q^2 < m_b^2$) regions.

For $m_{t'} > 300$ GeV, $\mathrm{Br}(B \to X_s l^+ l^-)$ is completely dominated by the Wilson coefficient C_{10}^{tot}. Hence in our numerical analysis, we neglect the small z-dependence in C_9^{tot}.

E. $B_q - \bar{B}_q$ mixing

Within SM, $B_q - \bar{B}_q$ mixing ($q = d, s$) proceeds to an excellent approximation only through the box diagrams with internal top quark exchanges. In case of four generations, there is an additional contribution to $B_q - \bar{B}_q$ mixing coming from the virtual exchange of the fourth generation up quark t'. The mass difference ΔM_q in SM4 is given by

$$\Delta M_q = 2|M_{12}|, \quad (25)$$

where

$$M_{12} = \frac{G_F^2 m_W^2}{12\pi^2} m_{B_q} B_{bq} f_{B_q}^2 \{\eta_t (V_{tq} V_{tb}^*)^2 S_0(x_t) + \eta_{t'} (V_{t'q} V_{t'b}^*)^2 S_0(x_{t'}) + 2\eta_{tt'} (V_{tq} V_{tb}^*) \times (V_{t'q} V_{t'b}^*) S_0(x_t, x_{t'})\}, \quad (26)$$

where $x_t = m_t^2/m_W^2$, $x_{t'} = m_{t'}^2/M_W^2$ and

$$S_0(x_t) = \frac{4x_t - 11x_t^2 + x_t^3}{4(1-x_t)^2} - \frac{3}{2}\frac{x_t^3 \ln x_t}{(1-x_t)^3}, \quad (27)$$

$$S_0(x_{t'}) = S_0(x_t \to x_{t'}), \quad (28)$$

$$S_0(x_t, x_{t'}) = x_t x_{t'} \left\{ \frac{\ln x_{t'}}{x_{t'} - x_t} \left[\frac{1}{4} + \frac{3}{2}\frac{1}{1-x_{t'}} - \frac{3}{4}\frac{1}{(1-x_{t'})^2} \right] - \frac{\ln x_t}{x_{t'} - x_t} \left[\frac{1}{4} + \frac{3}{2}\frac{1}{1-x_t} - \frac{3}{4}\frac{1}{(1-x_t)^2} \right] - \frac{3}{4}\frac{1}{(1-x_t)(1-x_{t'})} \right\}. \quad (29)$$

Here η_t is the QCD correction factor and its value is 0.5765 ± 0.0065 [54]. The QCD correction factor $\eta_{t'}$ is given by [66]

$$\eta_{t'} = (\alpha_s(m_t))^{6/23} \left(\frac{\alpha_s(m_{b'})}{\alpha_s(m_t)} \right)^{6/21} \left(\frac{\alpha_s(m_{t'})}{\alpha_s(m_{b'})} \right)^{6/19}. \quad (30)$$

$\alpha_s(\mu)$ is the running coupling constant at the scale μ at NLO [67]. Here we assume $\eta_{t'} = \eta_{tt'}$ for simplicity. The numerical values of the structure functions $S_0(x_{t'})$, $S_0(x_t, x_{t'})$ and the QCD correction factor $\eta_{t'}$ are given in Tables III and IV respectively for various t' mass.

F. Indirect CP violation in $K_L \to \pi\pi$

Indirect CP violation in $K_L \to \pi\pi$ is described by the parameter ϵ_K, the working formula for it is given by [68]

$$\epsilon_K = \exp(i\phi_\epsilon) \sin\phi_\epsilon (\mathrm{Im} M_{12}^k / \Delta M_k + \zeta), \quad (31)$$

where $\zeta = \frac{\mathrm{Im}A_0}{\mathrm{Re}A_0}$ with $A_0 \equiv A(K \to (\pi\pi)_{I=0})$ and ΔM_K denoting the $K_L - K_S$ mass difference. The off-diagonal element M_{12} in the neutral K-meson mass matrix represents $K^0 - \bar{K}^0$ mixing and is given by

$$M_{12}^* = \frac{\langle \bar{K}^0 | \mathcal{H}_{\mathrm{eff}}(\Delta S = 2) | K^0 \rangle}{2m_K} \quad (32)$$

The phase ϕ_ϵ is given by

$$\phi_\epsilon = (43.51 \pm 0.05)^\circ \quad (33)$$

The second term in Eq. (31) constitutes a $\mathcal{O}(5)\%$ correction to ϵ_K. In most of the phenomenological analysis ϕ_ϵ is taken as $\pi/4$ and ζ is taken as zero. However, $\zeta \neq 0$ and $\phi_\epsilon < \pi/4$ results in a suppression effect in ϵ_k relative to the approximate formula with $\zeta = 0$ and $\phi_\epsilon = \pi/4$. In order to include these corrections we have used the parametrization

$$\kappa_\epsilon = \sqrt{2} \sin\phi_\epsilon \bar{\kappa}_\epsilon, \quad (34)$$

where $\bar{\kappa}_\epsilon = 0.94 \pm 0.02$ and consequently $\kappa_\epsilon = 0.92 \pm 0.02$, $\bar{\kappa}_\epsilon$ parametrizing the effect of $\zeta \neq 0$ [68].

After some calculations it can be shown that [64]

$$M_{12} = \frac{G_F^2}{12\pi^2} f_K^2 B_K m_K M_W^2 [\lambda_c^{*2} \eta_c S_0(x_c) + \lambda_t^{*2} \eta_t S_0(x_t) + 2\lambda_c^* \lambda_t^* \eta_{ct} S_0(x_c, x_t) + \lambda_{t'}^{*2} \eta_{t'} S_0(x_{t'}) + 2\lambda_c^* \lambda_{t'}^* \eta_{ct'} S_0(x_c, x_{t'}) + 2\lambda_t^* \lambda_{t'}^* \eta_{tt'} S_0(x_t, x_{t'})], \quad (35)$$

where $\lambda_i = \lambda_{is}^* \lambda_{id}$ and $x_q = (m_q^2/M_W^2)$ for all quarks q.

Inserting (35) and (34) in (31) one finds

$$\epsilon_K = \frac{G_F^2}{12\pi^2 \sqrt{2} \Delta M_K} \kappa_\epsilon f_K^2 B_K m_K M_W^2 \, \mathrm{Im}[\lambda_c^{*2} \eta_c S_0(x_c) + \lambda_t^{*2} \eta_t S_0(x_t) + 2\lambda_c^* \lambda_t^* \eta_{ct} S_0(x_c, x_t) + \lambda_{t'}^{*2} \eta_{t'} S_0(x_{t'}) + 2\lambda_c^* \lambda_{t'}^* \eta_{ct'} S_0(x_c, x_{t'}) + 2\lambda_t^* \lambda_{t'}^* \eta_{tt'} S_0(x_t, x_{t'})], \quad (36)$$

where $f_K = 160$ MeV. The value for B_K has been taken from Ref. [50], in a recent analysis [69,70] the error has been reduced to $\lesssim 4\%$, however, in our analysis we use the more conservative value mentioned in Table III from [50].

G. $K^+ \to \pi^+ \nu \bar{\nu}$ decay

The effective Hamiltonian for $K^+ \to \pi^+ \nu \bar{\nu}$ can be written as

$$\mathcal{H}_{\mathrm{eff}} = \frac{G_F}{\sqrt{2}} \frac{\alpha}{2\pi \sin^2\Theta_w} \sum_{l=e,\mu,\tau} [V_{cs}^* V_{cd} X_{\mathrm{NL}}^l + V_{ts}^* V_{td} X(x_t) + V_{t's}^* V_{t'd} X(x_{t'})] (\bar{s}d)_{V-A} (\bar{\nu}_l \nu_l)_{V-A}. \quad (37)$$

The first term is the contribution from the charm sector.

TABLE III. The structure functions $S_0(x_{t'})$ and $S_0(x_t, x_{t'})$.

$m_{t'}$ (GeV)	400	600
$S_0(x_{t'})$	9.225	17.970
$S_0(x_t, x_{t'})$	4.302	5.225

TABLE IV. The QCD correction factor $\eta_{t'}$.

$m_{t'}$ (GeV)	400	600
$\eta_{t'}$	0.522	0.514

The function $X(x)$ is relevant for the top part,

$$X(x) = X_0(x) + \frac{\alpha_s}{4\pi} X_1(x), \tag{38}$$

where $x_q = (m_q^2/M_W^2)$ for all quarks q. Here $X_0(x)$ is the leading contribution given by

$$X_0(x) = \frac{x}{8}\left[-\frac{2+x}{1-x} + \frac{3x-6}{(1-x)^2}\ln x\right], \tag{39}$$

and $X_1(x)$ is the QCD correction. The expression for $X_1(x)$ is given in [64]. The function X can also be written as

$$X(x_{t/t'}) = \eta_X . X_0(x_{t/t'}), \qquad \eta_X = 0.994. \tag{40}$$

Here η_X represents the NLO corrections.

The function $X_{\rm NL}^l$ is the function corresponding to $X(x_t)$ in the charm sector. It results from the NLO calculations and its explicit form is given in [67,71].

The branching fraction of $K^+ \to \pi^+ \nu\bar{\nu}$ can be written as follows

$$\begin{aligned}\mathrm{Br}(K^+ \to \pi^+ \nu\bar{\nu}) = \kappa_+\bigg[&\left(\frac{\mathrm{Im}\lambda_t}{\lambda^5}X(x_t) + \frac{\mathrm{Im}\lambda_{t'}}{\lambda^5}X(x_{t'})\right)^2 \\ &+ \left(\frac{\mathrm{Re}\lambda_c}{\lambda}P_0(X) + \frac{\mathrm{Re}\lambda_t}{\lambda^5}X(x_t) \right.\\ &\left.+ \frac{\mathrm{Re}\lambda_{t'}}{\lambda^5}X(x_{t'})\right)^2\bigg],\end{aligned} \tag{41}$$

where

$$\kappa^+ = r_{K^+}\frac{3\alpha^2\,\mathrm{Br}(K^+ \to \pi^0 e^+ \nu)}{2\pi^2 \sin^4\Theta_W}\lambda^8, \tag{42}$$

$$P_0(X) = \frac{1}{\lambda^4}\left[\frac{2}{3}X_{\rm NL}^e + \frac{1}{3}X_{\rm NL}^\tau\right], \tag{43}$$

and $r_{K^+} = 0.901$ summarizes the isospin breaking corrections in relating the $K^+ \to \pi^+ \nu\bar{\nu}$ to the well-measured leading decay $K^+ \to \pi^0 e^+ \nu$.

III. PREDICTIONS IN THE SM4

Figure 1 (left panel) shows the correlations between the CP asymmetries in $B_d \to \phi K_s$ and $B_s \to \psi\phi$ whereas the right panel shows the variation $S_{\psi\phi}$ with the new phase $\phi_s'^2$; which has already been shown in our previous article [15] for $m_{t'} = 400$, 500, and 600 GeV; here, we have also included in the plot $m_{t'} = 300$ GeV. This is to clarify the fact that the present data on CP asymmetries tends to favor a fourth family of quarks with $m_{t'}$ in the range (400–600) GeV. In this article, therefore, we will focus mostly on $m_{t'} \approx 400$–600 GeV when we provide numerical results for SM4 for some interesting observables related to B and K systems which could be tested experimentally.

[2] Soon after we posted version 1 of our paper, [72] appeared which also discusses about the phenomenology of SM4. To facilitate direct comparison with that work we are adding few extra figures in this revised version.

A. Direct CP asymmetry in $B \to X_s\gamma$

A_{CP} in $B \to X_s\gamma$ is defined as

$$A_{CP}^{B\to X_s\gamma} = \frac{\Gamma(\bar{B} \to X_s\gamma) - \Gamma(B \to X_{\bar{s}}\gamma)}{\Gamma(\bar{B} \to X_s\gamma) + \Gamma(B \to X_{\bar{s}}\gamma)} \tag{44}$$

Within the SM, $A_{CP}^{B\to X_s\gamma}$ is predicted to be less than 1% [73–75]. The most recent SM prediction is [76] (Here we have calculated the errors by adding all errors given in the mentioned reference in quadrature)

$$A_{CP}^{B\to X_s\gamma}|_{E_\gamma > 1.6\,\mathrm{GeV}} = (0.44^{+0.24}_{-0.13})\%. \tag{45}$$

The current world average of $A_{CP}^{B\to X_s\gamma}$ is $(-1.2 \pm 2.8)\%$ [60], which is consistent with zero or a very small direct CP asymmetry as we have in the SM. The present experimental uncertainty is still an order of magnitude greater than the theoretical error. However, a dramatic improvement in the experimental sensitivity is possible at the upcoming Super-B factories and sensitivity of about 0.4%–0.5% can be achieved [77].

As the CP asymmetry within the SM is less than 1%, observation of a sizable CP asymmetry would be a clean signal of new physics. It is expected that the new physics models with nonstandard CP-odd phases can enhance $A_{CP}^{B\to X_s\gamma}$ and hence we study $A_{CP}^{B\to X_s\gamma}$ within the framework of SM4.

The general expression for the CP asymmetry in $B \to X_s\gamma$ is [74]

$$\begin{aligned}A_{CP}^{B\to X_s\gamma} \simeq \frac{10^{-2}}{|C_7^{\rm tot}(m_b)|^2}\{&-1.82\,\mathrm{Im}[C_7^{\rm new}] + 1.72\,\mathrm{Im}[C_8^{\rm new}] \\ &- 4.46\,\mathrm{Im}[C_8^{\rm new}C_7^{\rm new*}] \\ &+ 3.21\,\mathrm{Im}[\epsilon_s(1 - 2.18C_7^{\rm new*} - 0.26C_8^{\rm new*})]\},\end{aligned} \tag{46}$$

where

$$\epsilon_s = \frac{V_{us}^* V_{ub}}{V_{ts}^* V_{tb}}, \tag{47}$$

Here the new physics Wilson coefficients $C_{7,8}^{\rm new}$ are at scale M_W. In SM4,

$$C_{7,8}^{\rm new} = \frac{V_{t's}^* V_{t'b}}{V_{ts}^* V_{tb}} C_{7,8}^{t'}(M_W). \tag{48}$$

In Fig. 2 we have shown the correlation between CP asymmetries in $(B \to X_s\gamma)$ and $B_s \to J/\psi\phi$ $(S_{\psi\phi})$. The current 2σ experimental range for $S_{\psi\phi}$ is given by $[-0.90, -0.17]$ [78]. The SM value for $A_{CP}(B \to X_s\gamma)$ corresponds to $S_{\psi\phi} \approx 0$ or in other words $\phi_s^{t'} \approx 0$. It is easy to understand the nature of the plot i.e. decrease of $A_{CP}(B \to X_s\gamma)$ with increase of $S_{\psi\phi}$. From the expression for $A_{CP}(B \to X_s\gamma)$ [Eq. (46)], it is clear that in SM the only contribution to A_{CP} will come from the first part of the fourth term. In the presence of new phase and new cou-

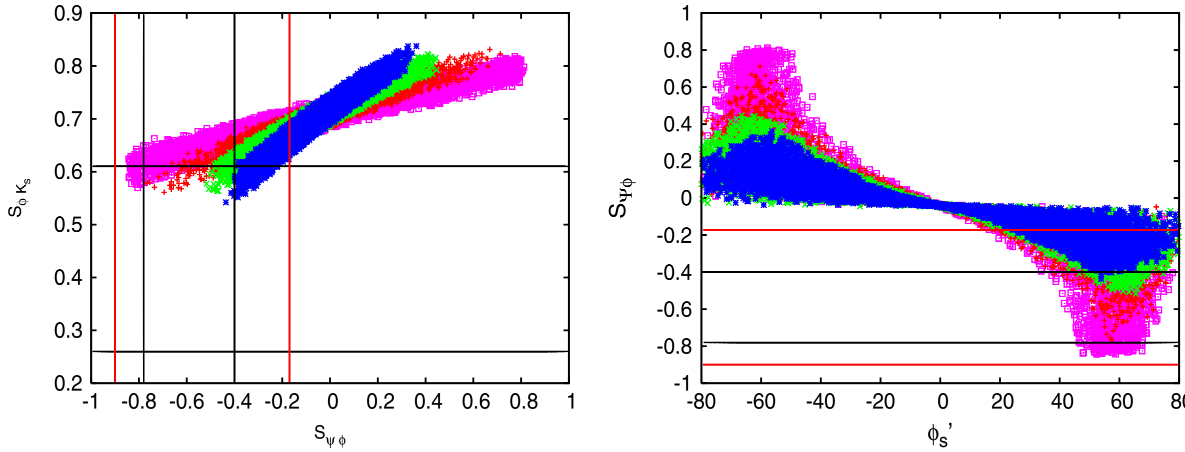

FIG. 1 (color online). (a) Correlation between $S_{\phi K_s}$ and $S_{\psi\phi}$ (left panel) and (b) Variation of $S_{\psi\phi}$ with the phase ϕ_s' of $\lambda_{t'}^s$ (right panel), for $m_{t'} = 300$ (magenta), 400 (red), 500 (green), and 600 (blue) GeV, respectively. The horizontal lines (left panel) represent the experimental 1σ range for $S_{\phi K_s}$ whereas the vertical lines (black 1-σ and red 2-σ) represent that for $S_{\psi\phi}$; in the right panel the horizontal lines are for $S_{\psi\phi}$.

pling, the first two terms and the fourth term will contribute to A_{CP}. Contribution from the first two terms is always negative and increases (mod value) with the new physics coupling [within the new physics (NP) region in which we are interested] whereas the fourth term is always positive and it has very small increase with the new physics coupling or phase.

B. *CP* asymmetry in $B_s \to X_s \ell \nu$

In this section we shall concentrate on semileptonic *CP* asymmetry ($A_{\rm SL}$) in B_s system.[3] In general the *CP* asymmetry in semileptonic B_s decays defined as

$$A_{\rm SL} = \frac{\Gamma[\bar{B}_s^{\rm phys}(t) \to \ell^+ X] - \Gamma[B_s^{\rm phys}(t) \to \ell^- X]}{\Gamma[\bar{B}_s^{\rm phys}(t) \to \ell^+ X] + \Gamma[B_s^{\rm phys}(t) \to \ell^- X]}, \quad (49)$$

depends on the relative phase between the absorptive and dispersive parts of $B_s - \bar{B}_s$ mixing amplitude [79]

$$A_{\rm SL} = {\rm Im}\left(\frac{\Gamma_{12}}{M_{12}}\right) = \frac{|\Gamma_{12}^s|}{|M_{12}^{\rm SM}|}\frac{\sin\phi_s}{|\Delta_s|}, \quad (50)$$

with $\phi_s = \arg(-\frac{M_{12}^s}{\Gamma_{12}^s})$, the relative phase between $B_s - \bar{B}_s$ mixing and the corresponding $b \to c\bar{c}s$ decays and $|\Delta_s|$ parametrizes the NP effect in M_{12}^s [6]. $|\Gamma_{12}/M_{12}| = O(m_b^2/M_W^2)$ suppresses $A_{\rm SL}$ to the percent level, apart from this there is a GIM suppression factor m_c^2/m_b^2 reducing $A_{\rm SL}$ by another order of magnitude. Because of these suppression factors it is very small in SM, for B_s system it is $\mathcal{O}(10^{-5})$. The GIM suppression is lifted if new physics contributes to $\arg(M_{12})$. Therefore, $A_{\rm SL}$ is very sensitive to new *CP* phases [80,81]. The situation where new physics could enhance $A_{\rm SL}$ by a factor $\mathcal{O}(10–100)$ makes this asymmetry a sensitive probe of new physics.

Recently the search for *CP* violation in semileptonic B_s decays achieved a much more improved sensitivity [82,83]:

$$\begin{aligned} A_{\rm SL} &= (2.45 \pm 1.96) \times 10^{-2} \\ {\rm D0} &= (2.00 \pm 2.79) \times 10^{-2} \quad {\rm CDF}. \end{aligned} \quad (51)$$

Present world average is given by [84],

$$A_{\rm SL} = (-0.37 \pm 0.94) \times 10^{-2} \quad {\rm HFAG}. \quad (52)$$

In near future more precise measurements can exclude SM

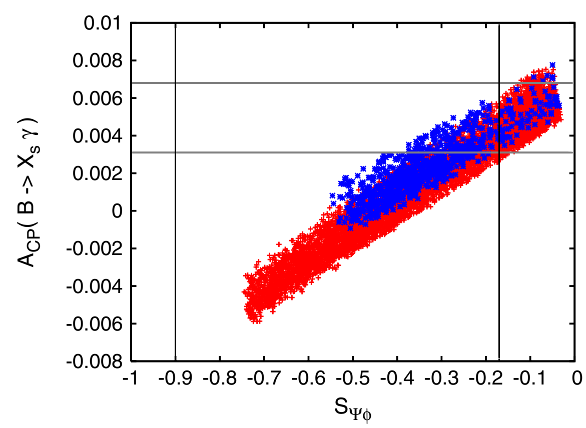

FIG. 2 (color online). Correlation between *CP* asymmetry in $B \to X_s \gamma$ and $S_{\psi\phi}$, the *CP* asymmetry in $B_s \to J/\psi\phi$; where the red and blue regions correspond to $m_{t'} = 400$ and 600 GeV whereas horizontal lines represent the SM limit for *CP* asymmetry and the vertical lines represent the 2σ limit for *CP* asymmetry in $B_s \to J/\psi\phi$.

[3]We were about to post a short paper reporting our study of $A_{\rm SL}$ in SM4 when the paper [72] appeared wherein this topic is also discussed; consequently we are making a very brief addition of this in version 2 of our paper. Our results agree with Buras *et al.* [72].

prediction if it is much enhanced then the SM prediction. It is important to note that the scenarios like SM4 can significantly affect M_{12}^s, but not Γ_{12}^s, which is dominated by the CKM-favored $b \to c\bar{c}s$ tree-level decays. The leading contribution to Γ_{12}^s was obtained in [79,85]. At present, Γ_{12}^s is known to next-to-leading-order (NLO) in both $\bar{\Lambda}/m_b$ [86] and $\alpha_s(m_b)$ [87–89], later in 2006 Nierste and Lenz [6] have improved the NLO calculation for $\Delta\Gamma_s$ and updated the value for $\Delta\Gamma_s$.

In Fig. 3 the sensitivity of semileptonic CP asymmetry to SM4 is shown and we note an enhancement by a factor of 100 from its SM prediction of order 10^{-5}. It could have a value -0.4% and -0.3% corresponding to maximum values of $S_{\psi\phi}$ for $m_{t'} = 400$ and 600 GeV, respectively.

C. CP asymmetry in $B \to X_s l^+ l^-$

It is very useful to consider new physics effects in the observables which are either zero or highly suppressed in the SM as they constitute null test of the SM [90]. The reason is that any finite or large measurement of such an observable may signal the existence of new physics. The CP asymmetry in $B \to X_s l^+ l^-$ is one such observable. In the SM, the CP asymmetry in $B \to X_s l^+ l^-$ is $\sim 10^{-3}$ [91,92]. In the SM, the only source of CP violation is the unique phase in the CKM quark mixing matrix. However in many possible extensions of the SM, there can be extra phases contributing to the CP asymmetry. Hence the CP asymmetry in $B \to X_s l^+ l^-$ is sensitive to SM4.

The CP asymmetry in $B \to X_s l^+ l^-$ is defined as

$$A_{CP}(z) = \frac{(d\mathrm{Br}/dz) - (d\overline{\mathrm{Br}}/dz)}{(d\mathrm{Br}/dz) + (d\overline{\mathrm{Br}}/dz)} = \frac{D(z) - \overline{D(z)}}{D(z) + \overline{D(z)}}, \quad (53)$$

where Br and $\overline{\mathrm{Br}}$ represent the branching ratio of $\bar{B} \to X_s l^+ l^-$ and its complex conjugate $B \to \bar{X}_s l^+ l^-$ respectively. $d\mathrm{Br}/dz$ is given in Eq. (21). The Wilson coefficients C_7^{tot}, C_9^{tot}, and C_{10}^{tot} can be written as

$$C_7^{\mathrm{tot}} = C_7(m_b) + \lambda_{tt'}^s C_7^{t'}(m_b), \quad (54)$$

$$C_9^{\mathrm{tot}} = \xi_1 + \lambda_{tu}^s \xi_2 + \lambda_{tt'}^s C_9^{t'}(m_b), \quad (55)$$

$$C_{10}^{\mathrm{tot}} = C_{10}(m_b) + \lambda_{tt'}^s C_{10}^{t'}(m_b), \quad (56)$$

where

$$\lambda_{tu}^s = \frac{\lambda_u^s}{\lambda_t^s} = \frac{V_{ub}^* V_{us}}{V_{tb}^* V_{ts}}, \quad (57)$$

$$\lambda_{tt'}^s = \frac{\lambda_{t'}^s}{\lambda_t^s} = \frac{V_{t'b}^* V_{t's}}{V_{tb}^* V_{ts}}, \quad (58)$$

so that all three relevant Wilson coefficients are complex in general. The parameters ξ_i are given by [63]

$$\begin{aligned}\xi_1 = {} & C_9(m_b) + 0.138\omega(z) + g(\hat{m}_c, z)(3C_1 + C_2 + 3C_3 \\ & + C_4 + 3C_5 + C_6) - \tfrac{1}{2} g(\hat{m}_d, z)(C_3 + 3C_4) \\ & - \tfrac{1}{2} g(\hat{m}_b, z)(4C_3 + 4C_4 + 3C_5 + C_6) \\ & + \tfrac{2}{9}(3C_3 + C_4 + 3C_5 + C_6), \end{aligned} \quad (59)$$

$$\xi_2 = [g(\hat{m}_c, z) - g(\hat{m}_u, z)](3C_1 + C_2). \quad (60)$$

Here

$$\begin{aligned}\omega(z) = {} & -\frac{2}{9}\pi^2 - \frac{4}{3}\mathrm{Li}_2(z) - \frac{2}{3}\ln z \ln(1 - z) \\ & - \frac{5 + 4z}{3(1 + 2z)}\ln(1 - z) - \frac{2z(1 + z)(1 - 2z)}{3(1 - z)^2(1 + 2z)}\ln z \\ & + \frac{5 + 9z - 6z^2}{6(1 - z)(1 + 2z)}, \end{aligned} \quad (61)$$

with

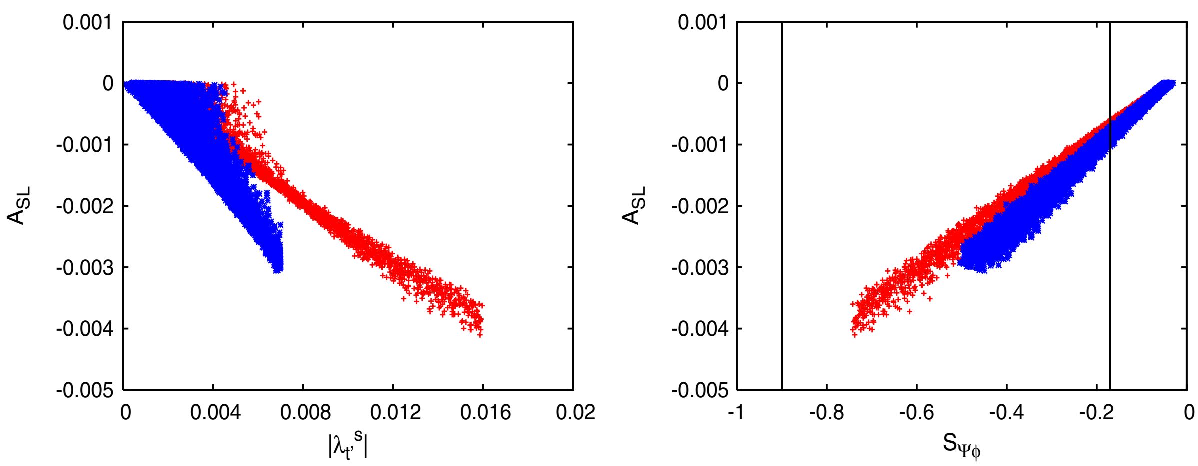

FIG. 3 (color online). Left panel shows the semileptonic CP asymmetry A_{SL} as a function of $|\lambda_{t'}^s|$ whereas in the right panel correlation between A_{SL} and $S_{\psi\phi}$ is shown; red and blue region corresponds to $m_{t'} = 400$ and 600 GeV, respectively, the SM value of A_{SL} (of order 10^{-5}) is too close to zero to be visible in the plot whereas the SM value for $S_{\psi\phi}$ is -0.04.

$$\mathrm{Li}_2(z) = -\int_0^z dt \frac{\ln(1-t)}{t}. \tag{62}$$

The function $g(\hat{m}, z)$ represents the one-loop corrections to the four-quark operators $O_1 - O_6$ and is given by [63]

$$g(\hat{m}, z) = -\frac{8}{9}\ln\frac{m_b}{\mu_b} - \frac{8}{9}\ln\hat{m} + \frac{8}{27} + \frac{4}{9}x - \frac{2}{9}(2+x)|1 - x|^{1/2}\begin{cases}\left(\ln\left|\frac{\sqrt{1-x}+1}{\sqrt{1-x}-1}\right| - i\pi\right), & \text{for } x \equiv \frac{4\hat{m}^2}{z} < 1\\ 2\arctan\frac{1}{\sqrt{x-1}}, & \text{for } x \equiv \frac{4\hat{m}^2}{z} > 1,\end{cases} \tag{63}$$

For light quarks, we have $\hat{m}_u \simeq \hat{m}_d \simeq 0$. In this limit,

$$g(0, z) = \frac{8}{27} - \frac{8}{9}\ln\frac{m_b}{\mu_b} - \frac{4}{9}\ln z + \frac{4}{9}i\pi. \tag{64}$$

We compute $g(\hat{m}, z)$ at $\mu_b = m_b$.

$d\overline{\mathrm{Br}}/dz$ can be obtained from dBr/dz by making the following replacements:

$$C_7^{\text{tot}} = C_7(m_b) + \lambda_{tt'}^s C_7^{t'}(m_b) \to \overline{C_7^{\text{tot}}} = C_7(m_b) + \lambda_{tt'}^{s*} C_7^{t'}(m_b), \tag{65}$$

$$C_9^{\text{tot}} = \xi_1 + \lambda_{tu}^s \xi_2 + \lambda_{tt'}^s C_9^{t'}(m_b) \to \overline{C_9^{\text{tot}}} = \xi_1 + \lambda_{tu}^{s*}\xi_2 + \lambda_{tt'}^{s*} C_9^{t'}(m_b), \tag{66}$$

$$C_{10}^{\text{tot}} = C_{10}(m_b) + \lambda_{tt'}^s C_{10}^{t'}(m_b) \to \overline{C_{10}^{\text{tot}}} = C_{10}(m_b) + \lambda_{tt'}^{s*} C_{10}^{t'}(m_b). \tag{67}$$

Then we get [93]

$$D(z) - \overline{D(z)} = 2\left(1 + \frac{2t^2}{z}\right)[\mathrm{Im}(\lambda_{tu}^s)\{2(1+2z)\,\mathrm{Im}(\xi_1\xi_2^*) - 12C_7\,\mathrm{Im}(\xi_2)\} + X_{im}\{(1+2z)C_9^{t'} + 6C_7^{t'}\}], \tag{68}$$

$$D(z) + \overline{D(z)} = \left(1 + \frac{2t^2}{z}\right)[(1+2z)\{B_1 + 2C_9^{t'}(|\lambda_{tt'}^s|^2 \times C_9^{t'} + X_{\text{re}})\} + 12\{B_2 + 2C_7C_9^{t'}\,\mathrm{Re}(\lambda_{tt'}^s) + C_7^{t'}(2|\lambda_{tt'}^s|^2 C_9^{t'} + X_{\text{re}})\}] + 8\left(1 + \frac{2t^2}{z}\right) \times \left(1 + \frac{2}{z}\right)|C_7^{\text{tot}}|^2 + 2\left[(1+2z) + \frac{2t^2}{z}(1-4z)\right]|C_{10}^{\text{tot}}|^2, \tag{69}$$

where

$$X_{\text{re}} = 2\{\mathrm{Re}(\lambda_{tt'}^s)\,\mathrm{Re}(\xi_1) + \mathrm{Re}(\lambda_{tt'}^s\lambda_{tu}^{s*})\,\mathrm{Re}(\xi_2)\}, \tag{70}$$

$$X_{\text{im}} = 2\{\mathrm{Im}(\lambda_{tt'}^s)\,\mathrm{Im}(\xi_1) + \mathrm{Im}(\lambda_{tt'}^s\lambda_{tu}^{s*})\,\mathrm{Im}(\xi_2)\}, \tag{71}$$

$$B_1 = 2\{|\xi_1|^2 + |\lambda_{tu}^s\xi_2|^2 + 2\,\mathrm{Re}(\lambda_{tu}^s)\,\mathrm{Re}(\xi_1\xi_2^*)\}, \tag{72}$$

$$B_2 = 2C_7\{\mathrm{Re}(\xi_1) + \mathrm{Re}(\lambda_{tu}^s)\,\mathrm{Re}(\xi_2)\}, \tag{73}$$

$$|C_{10}^{\text{tot}}|^2 = (C_{10})^2 + |\lambda_{tt'}^s|^2(C_{10}^{t'})^2 + 2C_{10}C_{10}^{t'}\,\mathrm{Re}(\lambda_{tt'}^s), \tag{74}$$

$$|C_7^{\text{tot}}|^2 = (C_7)^2 + |\lambda_{tt'}^s|^2(C_7^{t'})^2 + 2C_7C_7^{t'}\,\mathrm{Re}(\lambda_{tt'}^s). \tag{75}$$

From the expression for $g(\hat{m}, z)$ it is clear that the strong phase in $g(\hat{m}_{u/d}, z)$ and $g(\hat{m}_c, z)$ is responsible for CP asymmetry in $B \to X_s\ell^+\ell^-$ within the SM. $g(\hat{m}_{u/d}, z)$ is complex in both high and low-q^2 region whereas $g(\hat{m}_c, z)$ is complex only in the high-q^2 region. On the other hand, $g(\hat{m}_b, z)$ is always real. The SM CP asymmetry in high-q^2 region is almost zero since $\mathrm{Im}(\xi_2)$ is very small, almost one order in magnitude relative to its value in low-q^2 region, due to the relative cancellations of strong phases in ξ_2. In the presence of new physics, ξ_2 is unaffected but ξ_1 increases with the new physics coupling. On the other hand, we have contributions from the second term of Eq. (69) as a whole the CP asymmetry will increase with $S_{\psi\phi}$, as shown in the Fig. 4.

D. FB asymmetry in $B \to X_s l^+ l^-$

The quark level transition $b \to sl^+l^-$ is forbidden at the tree level within the SM and can occur only via one or more loops. Hence it has the potential to test higher order corrections to the SM and also to constrain many of its possible extensions. It gives rise to the inclusive decay $B \to X_s l^+ l^-$ which has been experimentally observed [94,95] with a branching ratio close to its SM predictions, $\mathrm{Br}(B \to X_s\ell^+\ell^-)(1 < q^2 < 6\ \mathrm{GeV}^2) = (1.63 \pm 0.20) \times 10^{-6}$

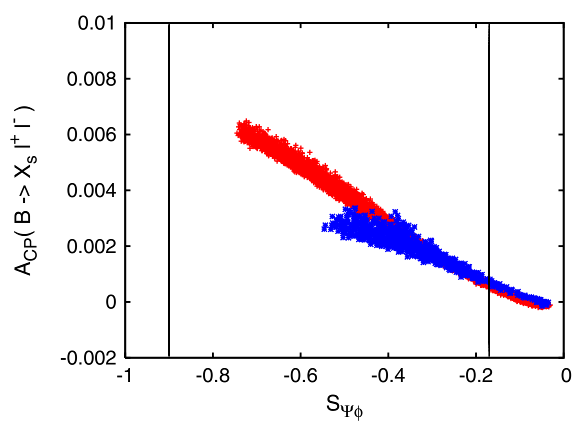

FIG. 4 (color online). Correlation between CP asymmetry in $B \to X_s\ell^+\ell^-$ (high-q^2 region) and $S_{\psi\phi}$. In the SM both the values are very small and in the plot they correspond to the point $[-0.04, 0.0]$. The red and blue regions correspond to $m_{t'} = 400$ and 600 GeV whereas the vertical lines represent 2σ experimental range for $S_{\psi\phi}$.

and $\mathrm{Br}(B \to X_s \ell^+ \ell^-)(q^2 > 14.4\,\mathrm{GeV}^2) = (3.84 \pm 0.75) \times 10^{-7}$ [96–98].

Apart from the branching ratio of semileptonic decay, there are other observables which are sensitive to new physics contribution to $b \to s$ transition. One such observable is FB asymmetry of leptons in $B \to X_s l^+ l^-$. The FB asymmetry of leptons in $B(p_b) \to X_s(p_s) l^+(p_{l^+}) l^-(p_{l^-})$ is obtained by integrating the double differential branching ratio ($d^2\mathrm{Br}/dz d\cos\theta$) with respect to the angular variable $\cos\theta$ [99]

$$A_{\mathrm{FB}}(z) = \frac{\int_0^1 d\cos\theta \frac{d^2\mathrm{Br}}{dz d\cos\theta} - \int_{-1}^0 d\cos\theta \frac{d^2\mathrm{Br}}{dz d\cos\theta}}{\int_0^1 d\cos\theta \frac{d^2\mathrm{Br}}{dz d\cos\theta} + \int_{-1}^0 d\cos\theta \frac{d^2\mathrm{Br}}{dz d\cos\theta}}, \quad (76)$$

where $z \equiv q^2/m_b^2 \equiv (p_{l^+} + p_{l^-})^2/m_b^2$ and θ is the angle between the momentum of the B-meson (or the outgoing s-quark) and that of l^+ in the center of mass frame of the dileptons $l^+ l^-$. FB asymmetry measures the difference in the right-chiral and left-chiral couplings of the leptonic current. FB asymmetry is driven by the top quark [99] and hence it is sensitive to the fourth generation up type quark t'.

Within the framework of SM4, the FB asymmetry in $B \to X_s l^+ l^-$ is given by

$$A_{\mathrm{FB}}(z) = -3\left(1 - \frac{4t^2}{z}\right)^{1/2} \frac{E(z)}{D(z)}, \quad (77)$$

where

$$E(z) = \mathrm{Re}(C_9^{\mathrm{tot}} C_{10}^{\mathrm{tot}*}) z + 2\,\mathrm{Re}(C_7^{\mathrm{tot}} C_{10}^{\mathrm{tot}*}), \quad (78)$$

and $D(z)$ is given in Eq. (22).

The FB asymmetry in $B \to X_s l^+ l^-$ becomes zero for a particular value of the dilepton invariant mass. Within SM, the zero of $A_{\mathrm{FB}}(q^2)$ appears in the low q^2 region, sufficiently away from the charm resonance region to allow the precise prediction of its position in perturbation theory. The value of the zero of the FB asymmetry is one of the most precisely calculated observables in flavor physics with a theoretical error of order 5%. The NNLO prediction for the zero of FB asymmetry is with $m_b = 4.8$ GeV [100]

$$(q^2)_0 = (3.5 \pm 0.12)\ \mathrm{GeV}^2. \quad (79)$$

This zero varies from model to model. Thus it can serve as an important probe to test SM4 experimentally.

As far as experiments are concerned, this quantity has not been measured as yet. But estimates show that a precision of about 5% could be obtained at Super-B factories [77].

From Fig. 5 one can see that the value of $z = \frac{q^2}{m_b^2}$, for which $A_{\mathrm{FB}}(z)$-asymmetry is zero, could be shifted to a lower value than its SM value (although it is consistent with the SM within the uncertainty). For $m_{t'} = 400$ and 600 GeV, one could have the value for $(q^2)_0$ ranging between $(3.09 \to 3.57)$ GeV^2 for $m_b = 4.8$ GeV.

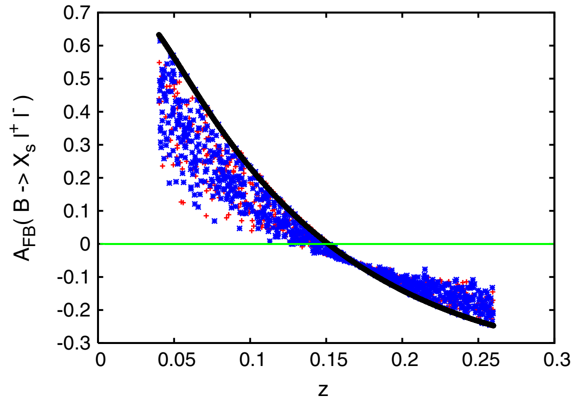

FIG. 5 (color online). Forward-backward (FB) asymmetry in $B \to X_s \ell^+ \ell^-$ has been plotted with $z = \frac{q^2}{m_b^2}$, the red and blue regions correspond to $m_{t'} = 400$ and 600 GeV, respectively, and the black thick line represents that for SM and the green line represents the zero of A_{FB}.

E. FB asymmetry in $B \to K^* \ell^+ \ell^-$

The quark level transition $b \to s\ell^+\ell^-$ is responsible for the exclusive decay $B \to K^* \ell^+ \ell^-$. The exclusive decay $B \to K^* \ell^+ \ell^-$ has relatively large theoretical errors as compared to the inclusive decay $b \to s\ell^+\ell^-$ due to the uncertainty in the determination of the hadronic form factors appearing in the transition amplitude $B \to K^*$. However, the exclusive decays are more readily accessible in the experiments. Therefore despite the large theoretical errors, the precise measurement of the exclusive decays could provide hints for possible deviations from the SM. The decay $B \to K^* \ell^+ \ell^-$ has been observed at the *BABAR* and Belle experiments [101–103]. Within the present experimental and theoretical precisions, the measured branching ratio is in agreement with the SM prediction [97,104]. However the measurements of the invariant dilepton mass is sparse. It is expected that the precise measurements of the Dalitz distributions in $B \to K^* \ell^+ \ell^-$ is possible at the LHCb and at the Super B factories. In particular, the measurement of FB asymmetry in $B \to K^* \ell^+ \ell^-$ is of great importance. This is because the uncertainty due to the form factors is minimal [105].

Within the SM4, the normalized FB asymmetry in $B \to K^* \ell^+ \ell^-$ is given by [105]

$$A_{\mathrm{FB}}(z) = -\frac{G_F^2 \alpha^2 m_B^4}{2^8 \pi^5 (d\Gamma/dz)} |V_{ts}^* V_{tb}|^2 z \lambda \left(1 - \frac{4\hat{m}_l^2}{z}\right) \times \left[\mathrm{Re}(C_9^{\mathrm{tot}} C_{10}^{\mathrm{tot}*}) V A_1 + \frac{\hat{m}_b}{z} \mathrm{Re}(C_7^{\mathrm{tot}} C_{10}^{\mathrm{tot}*}) \times \{V T_2 (1 - \hat{m}_{K^*}) + A_1 T_1 (1 + \hat{m}_{K^*})\}\right], \quad (80)$$

where

$$\lambda = 1 + \hat{m}_{K^*}^4 + z^2 - 2z - 2\hat{m}_{K^*}^2(1+z), \tag{81}$$

$$z = \frac{q^2}{m_B^2}, \tag{82}$$

$$\hat{m}_{K^*} = \frac{m_{K^*}}{m_B}. \tag{83}$$

Here $(d\Gamma/dz)$ is the $B \to K^* \ell^+ \ell^-$ differential decay distributions and its detailed expression can be seen from Ref. [105]. The form factors A_i, V, T_i are calculated in the light cone QCD approach and their values are given in [105].

The zero of FB asymmetry is determined by the equation,

$$\mathrm{Re}\,(C_9^{\mathrm{eff}}(z_0)) = -2\frac{\hat{m}_b}{z_0}C_7^{\mathrm{eff}}\frac{1-z_0}{1+m_{K^*}^2 - z_0}, \tag{84}$$

where z_0 corresponds to the value of z for which FB asymmetry is zero, within SM the value of $(q^2)_0$ for $m_b = 4.8$ GeV is given by [105]

$$(q^2)_0 = z_0 M_B^2 = 2.88^{+0.44}_{-0.28}\ \mathrm{GeV}^2. \tag{85}$$

From the left panel of Fig. 6, it is clear that within the uncertainty, the zero of the FB asymmetry in the SM4 is consistent with the SM prediction.

In Table V we have made a comparative study between SM, SM4 and experimental ranges for $A_{\mathrm{FB}}(q^2)$ in different q^2 region and one could see that the SM and SM4 predictions are within the present experimental bound. One interesting feature of data is that for low q^2 (first two bins), the central value (with appreciable errors) of A_{FB} is positive whereas SM predicts negative A_{FB} for these bins. Note also that there are deviations between SM and SM4 predicted FB asymmetries in some regions of q^2, for example, q^2 (GeV^2) with values in between $(0.6 \to 1.0)$, $(6.0 \to 8.0)$, and $(16.5 \to 18.0)$ the lower limit of SM4 predicted values are lower in magnitude than that for SM predictions; these differences are more prominent for $m_{t'} = 600$ GeV (see Table V).

F. $B_s \to l^+ l^-$ decay

The purely leptonic decays $B_s \to l^+l^-$, where $l = e, \mu, \tau$, are chirally suppressed within the SM and hence have appreciably smaller branching ratios as compared to that of the semileptonic decays. The helicity suppression is more dominant in the case of $B_s \to e^+e^-$ and $B_s \to \mu^+\mu^-$ which have branching ratio of $\sim(7.7 \pm 0.74) \times 10^{-14}$ and $\sim(3.35 \pm 0.32) \times 10^{-9}$, respectively [106], within the SM. However, the suppression is evaded to some extent in the case of $B_s \to \tau^+\tau^-$ due to the large m_τ, which has a branching ratio of $\sim 10^{-7}$. These decays are yet to be observed experimentally. The present upper bound on $B_s \to e^+e^-$ and $B_s \to \mu^+\mu^-$ are [60]

$$\begin{aligned} \mathrm{Br}\,(B_s \to e^+e^-) &< 0.28 \times 10^{-6}, \\ \mathrm{Br}(B_s \to \mu^+\mu^-) &< 3.60 \times 10^{-8}. \end{aligned} \tag{86}$$

As far as the τ channel is concerned, the current experimental information is rather poor. Using the LEP data on $B \to \tau\nu$ decays, the indirect bound on $\mathrm{Br}(B_s \to \tau^+\tau^-)$ is obtained to be [107]

$$\mathrm{Br}\,(B_s \to \tau^+\tau^-) < 5\%. \tag{87}$$

Though the decay $B_s \to \tau^+\tau^-$ has relatively larger branching ratio compared to $B_s \to e^+e^-$ and $B_s \to \mu^+\mu^-$, its observation will also be extremely difficult as the reconstruction of τ is a very challenging task. However, the upcoming experiments at the LHC can reach the SM sensitivity of $B_s \to \mu^+\mu^-$ and hence it can serve as an important probe to test the SM and constrain many new physics models. The LHCb will be able to probe the SM predictions for $B_s \to \mu^+\mu^-$ at 3σ with 2 fb^{-1} of data [108] whereas the ATLAS and CMS will be able to recon-

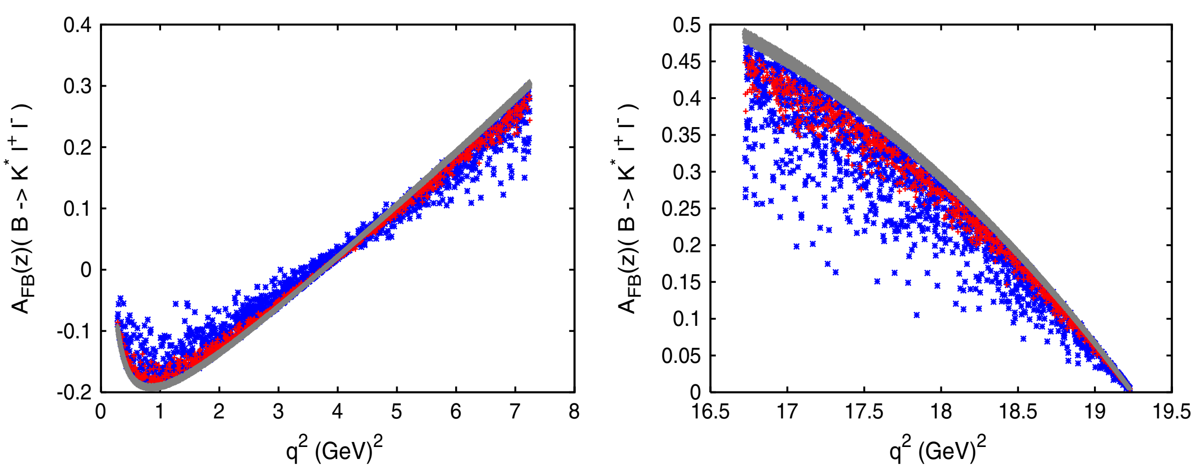

FIG. 6 (color online). FB-asymmetry in $B \to K^* \ell^+ \ell^-$ in the low-q^2 (left panel) and the high-q^2 region (right panel). The red and the blue regions correspond to $m_{t'} = 400$ and 600 GeV, respectively, and the grey region represents the SM prediction.

TABLE V. Values of FB asymmetry in different q^2 region.

q^2 (GeV$^2/c^2$)	$A_{\rm FB}$			
	exp	SM	$m_t' = 400$ GeV	$m_t' = 600$ GeV
0.6–1.0	$0.47^{+0.26}_{-0.33}$	$(-0.18 \to -0.19)$	$(-0.13 \to -0.19)$	$(-0.08 \to -0.19)$
1.0–6.0	$0.26^{+0.28}_{-0.31}$	$(-0.2 \to 0.2)$	$(-0.2 \to 0.2)$	$(-0.2 \to 0.2)$
6.0–8.0	$0.45^{+0.21}_{-0.26}$	$(0.19 \to 0.30)$	$(0.17 \to 0.28)$	$(0.11 \to 0.30)$
16.5–18.0	$0.66^{+0.12}_{-0.16}$	$(0.28 \to 0.49)$	$(0.25 \to 0.45)$	$0.15 \to 0.47$
18.0–19.5	For $(q^2 > 16)$	$(0.003 \to 0.30)$	$(0.003 \to 0.27)$	$0.003 \to 0.28$

struct the $B_s \to \mu^+\mu^-$ signal at 3σ with 30 fb^{-1} of data collection [109].

Here we study the decay $B_s \to \mu^+\mu^-$ and $B_s \to \tau^+\tau^-$ in the context of SM4.[4] Within the SM4, the branching ratio of $B_s \to l^+l^-$ is given by

$$\mathrm{Br}(B_s \to l^+l^-) = \frac{G_F^2\alpha^2 m_{B_s} m_l^2 f_{B_s}^2 \tau_{B_s}}{16\pi^3}|V_{tb}V_{ts}^*|^2 \times \sqrt{1-\frac{4m_l^2}{m_{B_s}^2}}|C_{10}^{\rm tot}|^2. \tag{88}$$

The branching ratio of $B_s \to l^+l^-$ can be predicted with higher accuracy by correlating it with the $B_s - \bar{B}_s$ mixing and then considerable uncertainty due to mixing angle and f_{B_s} gets removed. We have

$$\mathrm{Br}\,(B_s \to l^+l^-) = \frac{3\alpha^2\tau_{B_s}m_l^2}{8\pi B_{bs}m_W^2}\sqrt{1-\frac{4m_l^2}{m_{B_s}^2}}\frac{|C_{10}^{\rm tot}|^2}{|\Delta'|}\Delta M_s, \tag{89}$$

where B_{bs} is the "bag parameter" for B_s mesons for which the lattice result is given by [110],

$$B_{bs} = 1.33 \pm 0.06, \tag{90}$$

however, in order to be conservative we use the value 1.33 ± 0.15. In Eq. (89) the parameter Δ' is defined as

$$\Delta' = \left[\eta_t S_0(x_t) + \eta_{t'}\frac{(V_{t's}V_{t'b}^*)^2}{(V_{ts}V_{tb}^*)^2}S_0(x_{t'}) + 2\eta_{tt'}\frac{(V_{t's}V_{t'b}^*)}{(V_{ts}V_{tb}^*)}S_0(x_t, x_{t'})\right]. \tag{91}$$

In Fig. 7 we have shown the correlation between the branching fraction $\mathrm{Br}(B_s \to \ell^+\ell^-)$ and CP asymmetry in $B_s \to \psi\phi$, it is clear that there are possibilities for appreciably different predictions in SM4 compared to SM, enhanced or diminished by a factor of $\mathcal{O}(3)$. Note also that enhanced branching fractions correspond to a large CP asymmetry in $B_s \to \psi\phi$ and smaller branching fractions correspond to smaller asymmetry. The corresponding upper limit on the branching fractions are given by,

$$\begin{aligned}\mathrm{Br}(B_s \to \mu^+\mu^-) &< 8.0\times 10^{-9} \qquad m_{t'} = 400\ \text{GeV},\\ &< 1.2\times 10^{-8}, \qquad m_{t'} = 600\ \text{GeV},\\ \mathrm{Br}(B_s \to \tau^+\tau^-) &< 1.8\times 10^{-6} \qquad m_{t'} = 400\ \text{GeV},\\ &< 2.4\times 10^{-6}, \qquad m_{t'} = 600\ \text{GeV}.\end{aligned} \tag{92}$$

However, when $S_{\psi\phi}$ is close to its SM value, i.e. when the CP violating phase $\phi_{t'}^s$ of $V_{t's}$ is close to zero, the branching fractions reduce from their SM value since $|C_{10}^{\rm tot}|$ and δ' in Eq. (91) are reduced from its SM value due to destructive interference with SM4 counterpart.

G. Branching fraction $B \to X_s\nu\bar{\nu}$

The decays $B \to X_s\nu\bar{\nu}$ are the theoretically cleanest decays in the field of rare B-decays. They are dominated by the same Z^0-penguin and box diagrams involving top quark exchanges which we encounter in the case of $K_L \to \pi^0\nu\bar{\nu}$, since the change of the external quark flavors has no impact on the $m_{t/t'}$ dependence, the later is fully described by the function $X(x_{t/t'})$ which includes the NLO corrections. The charm contribution is negligible here. The effective Hamiltonian for the decay $B \to X_s\nu\bar{\nu}$ is given by [5]

$$\mathcal{H}_{\rm eff} = \frac{G_F}{\sqrt{2}}\frac{\alpha}{2\pi\sin^2\Theta_w}(V_{tb}^*V_{ts}X(x_t) + V_{t's}^*V_{t'd}X(x_{t'})) \times (\bar{b}s)_{V-A}(\bar{\nu}\nu)_{V-A} + \text{H.c.} \tag{93}$$

with

$$X(x) = \frac{x}{8}\left[\frac{2+x}{x-1} + \frac{3x-6}{(x-1)^2}\ln x\right]. \tag{94}$$

The calculation of the branching fractions for $B \to X_s\nu\bar{\nu}$ can be done in the spectator model corrected for short-distance QCD effects. Normalizing it to $\mathrm{Br}(B \to X_c\nu\bar{\nu})$ and summing over three neutrino flavors one finds [64,111]

[4] As mentioned in the introduction, the contribution to these processes from 4th generation heavy leptons is being neglected here.

[5] As mentioned in the introduction, the contribution to these processes from 4th generation heavy leptons is being neglected here.

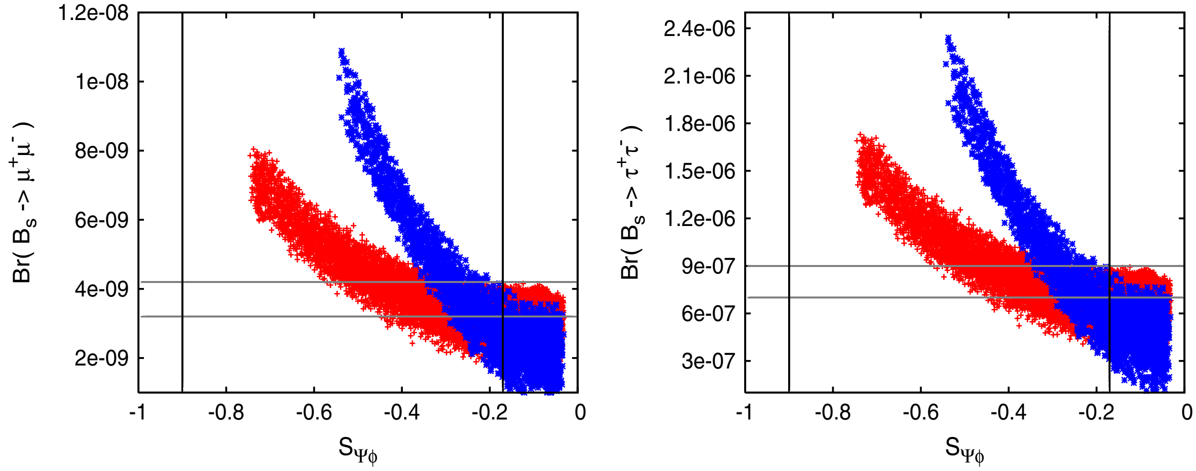

FIG. 7 (color online). Correlation between branching fraction in $B_s \to \mu^+\mu^-$ (left panel) and $B_s \to \tau^+\tau^-$ (right panel) with $S_{\psi\phi}$, where the red and blue regions correspond to $m_{t'} = 400$ and 600 GeV, respectively, the horizontal lines represent the SM limit for $\mathrm{Br}(B_s \to \ell^+\ell^-)$ whereas the vertical lines represent the 2σ experimental range for $S_{\psi\phi}$.

$$\frac{\mathrm{Br}(B \to X_s \nu\bar{\nu})}{\mathrm{Br}(B \to X_c e\bar{\nu})} = \frac{3\alpha^2}{4\pi^2 \sin^4\Theta_W} \frac{\bar{\eta}}{f(z)\kappa(z)} \frac{1}{|V_{cb}|^2} |\lambda_t X(x_t) + \lambda_{t'} X(x_{t'})|^2 = \frac{\tilde{C}^2 \bar{\eta}}{|V_{cb}|^2 f(z)\kappa(z)}, \tag{95}$$

where

$$\tilde{C}^2 = (\tilde{C}^{\mathrm{SM}})^2 \left| 1 + \frac{V^*_{t'b} V_{t's}}{V^*_{tb} V_{ts}} \frac{X_0(x_{t'})}{X_0(x_t)} \right|^2, \tag{96}$$

with

$$(\tilde{C}^{\mathrm{SM}})^2 = \frac{\alpha^2}{2\pi^2 \sin^4\Theta_W} |V^*_{tb} V_{ts} X_0(x_t)|^2. \tag{97}$$

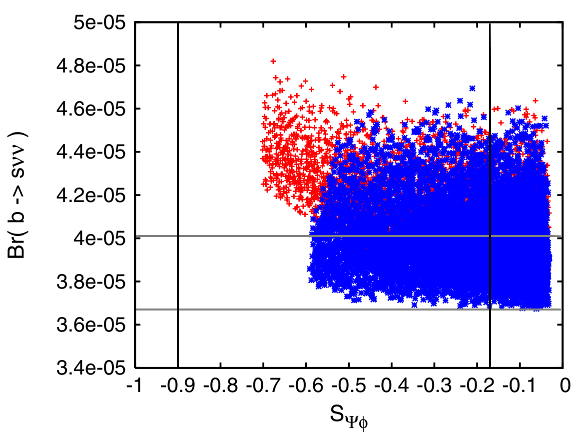

FIG. 8 (color online). Correlation between branching fraction in $B \to X_s \nu\bar{\nu}$ and $S_{\psi\phi}$, where the red and blue regions correspond to $m_{t'} = 400$ and 600 GeV, respectively, the horizontal lines represent the SM limit for $\mathrm{Br}(B \to X_s \nu\bar{\nu})$ whereas the vertical lines represent the 2σ experimental range for $S_{\psi\phi}$.

The factor $\bar{\eta}$ represents the QCD correction to the matrix element of the $b \to s\nu\bar{\nu}$ transition due to virtual and bremsstrahlung contributions and is given by the well-known expression

$$\bar{\eta} = \kappa(0) = 1 + \frac{2\alpha_s(m_b)}{3\pi}\left(\frac{25}{4} - \pi^2\right) \approx 0.83. \tag{98}$$

The SM4 predicted branching fraction (Fig. 8) $\mathrm{Br}(B \to X_s \nu\bar{\nu})$ could be sufficiently larger than its SM limit, $(3.66 \to 4.01) \times 10^{-5}$ [64] within the uncertainties, for values of $S_{\psi\phi}$ sufficiently away from its SM predictions. We are constraining $\lambda^s_t = V_{tb} V^*_{ts}$ using CKM4 unitarity with $\lambda^s_{t'} = V_{t'b} V^*_{t's}$ as free parameter, with the change of phase and amplitude of $\lambda^s_{t'}$, $|\lambda^s_t|$ increases from its SM value resulting an overall enhancement of $\mathrm{Br}(B \to X_s \nu\bar{\nu})$ from its SM prediction. For values of $\phi^s_{t'}$ close to 80°, the terms within modulus in Eq. (96) and (97) have their maximum values and so the branching fraction is sufficiently larger than its SM prediction and reach its maximum value 4.8×10^{-5}. In passing, we note incidentally that the upper limit that we have obtained for SM4 is consistent with that obtained in Ref. [112], in models with minimal flavor violation (MFV), and with the present experimental bound 6.4×10^{-4} [113].

H. Branching fraction $K^+ \to \pi^+\nu\bar{\nu}$

Although we have taken branching fraction for $K^+ \to \pi^+\nu\bar{\nu}$ as a constrain to fit V_{CKM4}, in Fig. 9 we show the effect of SM4; note that in the left panel only the 1σ range for the branching fraction using the constraints given in the Table I [except $\mathrm{Br}(K^+ \to \pi^+\nu\bar{\nu})$] is shown.[6]

[6]The right panel is added in our version 2 to facilitate direct comparison with [72].

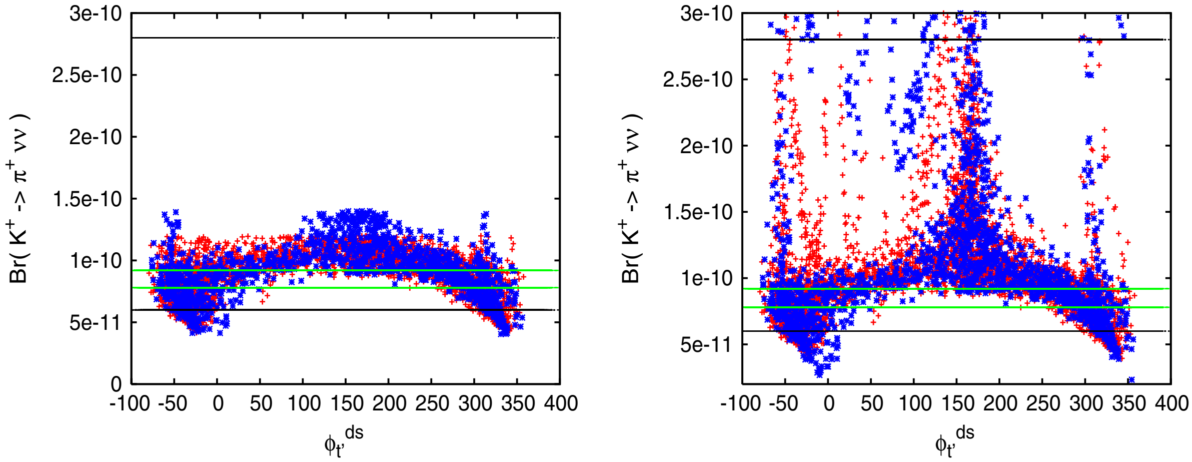

FIG. 9 (color online). Plot between the branching fraction of $K^+ \to \pi^+ \nu\bar{\nu}$ with $\phi_{t'}^{ds} = \phi_{t'}^{d} - \phi_{t'}^{s}$ bounded by the present experimental limit, red and blue region corresponds to $m_{t'} = 400$ and 600 GeV, respectively, the green and black horizontal lines represent 1σ limit for SM and experimental value, respectively. Left panel shows only 1σ range expected in SM4; full range is shown in the right panel.

From Fig. 9 one could see that the $\mathrm{Br}(K^+ \to \pi^+ \nu\bar{\nu})$ could be enhanced to its present experimental upper limit. In order to understand the nature of the plot one needs to concentrate on Eq. (41), and it is important to note that $\mathrm{Br}(K^+ \to \pi^+ \nu\bar{\nu})$ is dominated by the second term of the expression i.e. the term proportional to $\mathrm{Re}(\lambda_q)$ it should also be noted that the SM and SM4 part for each term has a relative sign difference. When $\phi_{t'}^{ds}$ is negative [i.e. when $\phi_{t'}^{d}$ has values in between (0–80)°] and $\phi_{t'}^{ds} > 270°$ the branching fraction will decrease because of the destructive interference between SM and SM4 part in the second term of Eq. (41). For $\phi_{t'}^{ds}$ in between (90–180)° the branching fraction have values above the SM value it is due to constructive interference between SM and SM4 in the second term of Eq. (41).

Present NNLO predictions for branching fraction for $K^+ \to \pi^+ \nu\bar{\nu}$ within SM is given by [114]

$$\mathrm{Br}\,(K^+ \to \pi^+ \nu\bar{\nu}) = (8.5 \pm 0.7) \times 10^{-11}, \tag{99}$$

and the SM4 1σ limit on $\mathrm{Br}(K^+ \to \pi^+ \nu\bar{\nu})$ is given by

$$\begin{aligned} \mathrm{Br}(K^+ \to \pi^+ \nu\bar{\nu}) &= (4.0 \to 12.0) \times 10^{-11}; \\ m_{t'} &= 400\ \mathrm{GeV}, \\ \mathrm{Br}(K^+ \to \pi^+ \nu\bar{\nu}) &= (4.0 \to 13.0) \times 10^{-11}; \\ m_{t'} &= 600\ \mathrm{GeV}. \end{aligned} \tag{100}$$

Again these upper limits are consistent with the 95% confidence level limit obtained in Ref. [112] calculated in the MFV model.

I. Branching fraction $K_L \to \pi^0 \nu\bar{\nu}$

The effective Hamiltonian for $K_L \to \pi^0 \nu\bar{\nu}$ can be written as

$$\mathcal{H}_{\mathrm{eff}} = \frac{G_F}{\sqrt{2}} \frac{\alpha}{2\pi \sin^2\Theta_w} (V_{ts}^* V_{td} X(x_t) + V_{t's}^* V_{t'd} X(x_{t'})) \times (\bar{s}d)_{V-A} (\bar{\nu}\nu)_{V-A} + \mathrm{H.c.} \tag{101}$$

Within SM $K_L \to \pi^0 \nu\bar{\nu}$ decay, proceeds almost entirely through *CP* violation, is completely dominated by short-distance loop diagrams with top quark exchanges, here the charm contribution can be fully neglected.

The branching fraction of $K_L \to \pi^0 \nu\bar{\nu}$ can be written as follows

$$\mathrm{Br}\,(K_L \to \pi^0 \nu\bar{\nu}) = \kappa_L . \left[\left(\frac{\mathrm{Im}\lambda_t}{\lambda^5} X(x_t) + \frac{\mathrm{Im}\lambda_{t'}}{\lambda^5} X(x_{t'}) \right)^2 \right], \tag{102}$$

with

$$\kappa_L = \frac{r_{K_L}}{r_{K^+}} \frac{\tau(K_L)}{\tau(K^+)} \kappa_+ = 1.80 \times 10^{-10}, \tag{103}$$

κ_+ and $r_{K_L} = 0.944$ summarizing isospin breaking corrections in relating $K_L \to \pi^0 \nu\bar{\nu}$ to $K^+ \to \pi^0 e^+ \nu$. The current value of branching fraction for $K_L \to \pi^0 \nu\bar{\nu}$ with SM is given by [114]

$$\mathrm{Br}\,(K_L \to \pi^0 \nu\bar{\nu}) = (2.76 \pm 0.40) \times 10^{-11}. \tag{104}$$

In Fig. 10, the variation of branching fraction $\mathrm{Br}(K_L \to \pi^0 \nu\bar{\nu})$ with the phase $\phi_{t'}^{ds}$ is shown.[7] We note that with the constraint on $\mathrm{Br}(K^+ \to \pi^+ \nu\bar{\nu})$ (Table I), while, in principle $\mathrm{Br}(K_L \to \pi^0 \nu\bar{\nu})$ could be enhanced as much as 1.2×10^{-9} (right panel Fig. 10), the expected 1σ range in SM4 (left panel Fig. 10) is only to 7×10^{-11}, however, at 95% CL the value could be enhanced to 8×10^{-10}. The branch-

[7]The right panel is added in our revised version to facilitate direct comparison with [72].

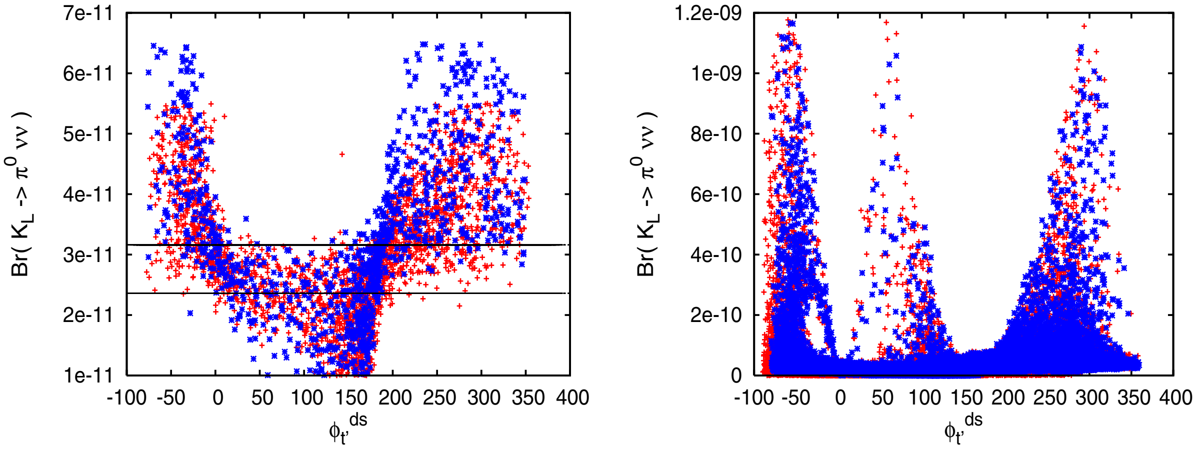

FIG. 10 (color online). The branching fraction of $K_L \to \pi^0 \nu \bar{\nu}$ versus $\phi_{t'}^{ds} = \phi_{t'}^{d} - \phi_{t'}^{s}$ in SM4, red and blue region corresponds to $m_{t'} = 400$ and 600 GeV, respectively, the black horizontal lines represent 1σ SM limit; left panel shows only 1σ range expected in SM4, full range for SM4 is shown in the right panel.

ing fraction has its maximum value when the phase $\phi_{t'}^{ds}$ has the value $\pm 90°$ and 270° since SM4 contribution picks up its maximum value at those points [Eq. (102)].

The SM4 1σ limit on $\mathrm{Br}(K_L \to \pi^0 \nu \bar{\nu})$ is given by

$$\begin{aligned} \mathrm{Br}(K_L \to \pi^0 \nu \bar{\nu}) &= (1.0 \to 5.2) \times 10^{-11}; \\ m_{t'} &= 400 \text{ GeV}, \\ \mathrm{Br}(K_L \to \pi^0 \nu \bar{\nu}) &= (1.0 \to 6.2) \times 10^{-11}; \\ m_{t'} &= 600 \text{ GeV}, \end{aligned} \tag{105}$$

the upper limits are consistent with the limit calculated in Ref. [112].

J. *CP* violation in $B \to \pi K$ modes

The observed data from the currently running two asymmetric B factories are almost consistent with the SM predictions and till now there is no compelling evidence for new physics. However, there are some interesting deviations from the SM associated with the $b \to s$ transitions, which provide us with possible indication of new physics. For example, the mixing induced *CP* asymmetries in many $b \to s\bar{q}q$ penguin-dominated modes do not seem to agree with the SM expectations. The measured values in such modes follow the trend $S_{s\bar{q}q} < \sin 2\beta$ [5,60], whereas in the SM they are expected to be similar [115,116]. In this context, $B \to \pi K$ decay modes, which receive dominant contributions from $b \to s$ mediated QCD penguins in the SM, provide another testing ground to look for new physics.

The first one is the difference in direct *CP* asymmetries in $B^- \to \pi^0 K^-$ and $\bar{B}^0 \to \pi^+ K^-$ modes. These two modes receive similar dominating contributions from tree and penguin diagrams and hence one would naively expect that these two channels will have the same direct *CP* asymmetries i.e., $\mathcal{A}_{\pi^0 K^-} = \mathcal{A}_{\pi^+ K^-}$. In the QCD factorization approach, the difference between these asymmetries is found to be [3]

$$\Delta A_{CP} = \mathcal{A}_{K^-\pi^0} - \mathcal{A}_{K^-\pi^+} = (2.5 \pm 1.5)\% \tag{106}$$

whereas the corresponding experimental value [60] is

$$\Delta A_{CP} = (14.8 \pm 2.8)\%, \tag{107}$$

which yields nearly 4σ deviation.

The second anomaly is associated with the mixing-induced *CP* asymmetry in $B^0 \to \pi^0 K^0$ mode. The time-dependent *CP* asymmetry in this mode is defined as

$$\begin{aligned} &\frac{\Gamma(\bar{B}^0(t) \to \pi^0 K_s) - \Gamma(B^0(t) \to \pi^0 K_s)}{\Gamma(\bar{B}^0(t) \to \pi^0 K_s) + \Gamma(B^0(t) \to \pi^0 K_s)} \\ &\quad = A_{\pi^0 K_s} \cos(\Delta M_d t) + S_{\pi^0 K_s} \sin(\Delta M_d t), \end{aligned} \tag{108}$$

and in the pure QCD penguin limit one expects $A_{\pi^0 K_s} \approx 0$ and $S_{\pi^0 K_s} \approx \sin(2\beta)$. Small nonpenguin contributions do provide some corrections to these asymmetry parameters and it has been shown in Refs. [117–119] that these corrections generally tend to increase $S_{K\pi^0}$ from its pure penguin limit of ($\sin 2\beta$) by a modest amount i.e., $S_{\pi^0 K_s} \approx 0.8$. Recently, using isospin symmetry it has been shown in [120–122] that the standard model favors a large $S_{\pi^0 K_s} \approx 0.99$.

However, the recent results from Belle [123] and *BABAR* [124] are

$$\begin{aligned} A_{\pi^0 K_s} &= 0.14 \pm 0.13 \pm 0.06, \\ S_{\pi^0 K_s} &= 0.67 \pm 0.31 \pm 0.08 \quad \text{(Belle)} \\ A_{\pi^0 K_s} &= -0.13 \pm 0.13 \pm 0.03, \\ S_{\pi^0 K_s} &= 0.55 \pm 0.20 \pm 0.03 \quad \text{(BABAR)} \end{aligned} \tag{109}$$

with average

$$A_{\pi^0 K_s} = -0.01 \pm 0.10, \qquad S_{\pi^0 K_s} = 0.57 \pm 0.17. \quad (110)$$

As seen from (110), the observed value of $S_{\pi^0 K_s}$ is found to be smaller than the present world average value of $\sin 2\beta = 0.672 \pm 0.024$ measured in $b \to c\bar{c}s$ transitions [60] by nearly 1σ and the deviation from the SM expectation given above is possibly even larger. This deviation which is opposite to the SM expectation, implies the possible presence of new physics in the $B^0 \to K^0\pi^0$ decay amplitude. In the SM, this decay mode receives contributions from QCD penguin (P), electroweak penguin ($P_{\rm EW}$), and color-suppressed tree (C) diagrams, which follow the hierarchical pattern $P{:}P_{\rm EW}{:}C = 1{:}\lambda{:}\lambda^2$, where $\lambda \approx 0.2257$ is the Wolfenstein expansion parameter. Thus, accepting the above discrepancy seriously one can see that the electroweak penguin sector is the best place to search for new physics.

To account for these discrepancies here we consider the effect of sequential fourth generation quarks [20,44–47]. In the SM, the relevant effective Hamiltonian describing the decay modes $B \to \pi K$ is given by

$$\mathcal{H}_{\rm eff}^{\rm SM} = \frac{G_F}{\sqrt{2}}\left[V_{ub}V_{us}^*(C_1O_1 + C_2O_2) - V_{tb}V_{ts}^*\sum_{i=3}^{10} C_iO_i\right]. \quad (111)$$

With a sequential fourth generation, the Wilson coefficients C_i's will be modified due to the new contributions from t' quark in the loop. Furthermore, due to the presence of the t' quark the unitarity condition becomes $\lambda_u + \lambda_c + \lambda_t + \lambda_{t'} = 0$, where $\lambda_q = V_{qb}V_{qs}^*$.

Thus, including the fourth generation and replacing $\lambda_t = -(\lambda_u + \lambda_c + \lambda_{t'})$, the modified Hamiltonian becomes

$$\begin{aligned}\mathcal{H}_{\rm eff} &= \frac{G_F}{\sqrt{2}}\bigg[\lambda_u(C_1O_1 + C_2O_2) \\ &\quad - \lambda_t\sum_{i=3}^{10} C_iO_i - \lambda_{t'}\sum_{i=3}^{10} C_i^{t'}O_i\bigg] \\ &= \frac{G_F}{\sqrt{2}}\bigg[\lambda_u\bigg(C_1O_1 + C_2O_2 + \sum_{i=3}^{10} C_iO_i\bigg) \\ &\quad + \lambda_c\sum_{i=3}^{10} C_iO_i - \lambda_{t'}\sum_{i=3}^{10} \Delta C_iO_i\bigg],\end{aligned} \quad (112)$$

where ΔC_i's are the effective (t subtracted) t' contributions.

Thus, one can obtain the transition amplitudes in the QCD factorization approach as [39,40]

$$\begin{aligned}\sqrt{2}A(B^- \to \pi^0K^-) &= \lambda_u(A_{\pi\bar{K}}(\alpha_1 + \beta_2) + A_{\bar{K}\pi}\alpha_2) + \sum_{p=u,c}\lambda_p\bigg(A_{\pi\bar{K}}(\alpha_4^p + \alpha_{4,\rm EW}^p + \beta_3^p + \beta_{3,\rm EW}^p) + \frac{3}{2}A_{\bar{K}\pi}\alpha_{3,\rm EW}^p\bigg) \\ &\quad - \lambda_{t'}\bigg(A_{\pi\bar{K}}(\Delta\alpha_4 + \Delta\alpha_{4,\rm EW} + \Delta\beta_3 + \Delta\beta_{3,\rm EW}) + \frac{3}{2}A_{\bar{K}\pi}\Delta\alpha_{3,EW}\bigg), \\ A(\bar{B}^0 \to \pi^+K^-) &= \lambda_u(A_{\pi\bar{K}}\alpha_1) + \sum_{p=u,c}\lambda_pA_{\pi\bar{K}}\bigg(\alpha_4^p + \alpha_{4,\rm EW}^p + \beta_3^p - \frac{1}{2}\beta_{3,\rm EW}^p\bigg) \\ &\quad - \lambda_{t'}A_{\pi\bar{K}}\bigg(\Delta\alpha_4 + \Delta\alpha_{4,\rm EW} + \Delta\beta_3 - \frac{1}{2}\Delta\beta_{3,\rm EW}\bigg), \\ \sqrt{2}A(\bar{B}^0 \to \pi^0\bar{K}^0) &= \lambda_uA_{\bar{K}\pi}\alpha_2 + \sum_{p=u,c}\lambda_p\bigg[A_{\pi\bar{K}}\bigg(-\alpha_4^p + \frac{1}{2}\alpha_{4,\rm EW}^p - \beta_3^p + \frac{1}{2}\beta_{3,\rm EW}^p\bigg) + \frac{3}{2}A_{\bar{K}\pi}\alpha_{3,\rm EW}^p\bigg] \\ &\quad - \lambda_{t'}\bigg[A_{\pi\bar{K}}\bigg(-\Delta\alpha_4 + \frac{1}{2}\Delta\alpha_{4,\rm EW} - \Delta\beta_3 + \frac{1}{2}\Delta\beta_{3,\rm EW}\bigg) + \frac{3}{2}A_{\bar{K}\pi}\Delta\alpha_{3,\rm EW}\bigg],\end{aligned} \quad (113)$$

where

$$\begin{aligned}A_{\pi\bar{K}} &= i\frac{G_F}{\sqrt{2}}M_B^2F_0^{B\to\pi}f_K \quad \text{and} \\ A_{\bar{K}\pi} &= i\frac{G_F}{\sqrt{2}}M_B^2F_0^{B\to K}f_\pi.\end{aligned} \quad (114)$$

These amplitudes can be symbolically represented as

$$\text{Amp} = \lambda_uA_u + \lambda_cA_c - \lambda_{t'}A_{t'}. \quad (115)$$

λ's contain the weak phase information and A_i's are associated with the strong phases. Thus one can explicitly separate the strong and weak phases and write the amplitudes as

$$\text{Amp} = \lambda_cA_c[1 + rae^{i(\delta_1-\gamma)} - r'be^{i(\delta_2+\phi_s)}], \quad (116)$$

where $a = |\lambda_u/\lambda_c|$, $b = |\lambda_{t'}/\lambda_c|$, $-\gamma$ is the weak phase of V_{ub} and ϕ_s is the weak phase of $\lambda_{t'}$. $r = |A_u/A_c|$, $r' = |A_{t'}/A_c|$, and δ_1 (δ_2) is the relative strong phases between A_u and A_c ($A_{t'}$ and A_c). From these amplitudes one can obtain the direct and mixing induced CP asymmetry parameters as

$$A_{\pi K} = \frac{2[ra\sin\delta_1\sin\gamma + r'b\sin\delta_2\sin\phi_s + rr'ab\sin(\delta_2-\delta_1)\sin(\gamma+\phi_s)]}{[\mathcal{R} + 2ra\cos\delta_1\cos\gamma - 2r'b\cos\delta_2\cos\phi_s - 2rr'ab\cos(\delta_2-\delta_1)\cos(\gamma+\phi_s)]},$$
$$S_{\pi K} = \frac{X}{\mathcal{R} + 2ra\cos\delta_1\cos\gamma - 2r'b\cos\delta_2\cos\phi_s - 2rr'ab\cos(\delta_2-\delta_1)\cos(\gamma+\phi_s)}, \tag{117}$$

where $\mathcal{R} = 1 + (ra)^2 + (r'b)^2$ and

$$\begin{aligned} X = {} & \sin 2\beta + 2ra\cos\delta_1\sin(2\beta+\gamma) \\ & - 2r'b\cos\delta_2\sin(2\beta-\phi_s) + (ra)^2\sin(2\beta+2\gamma) \\ & + (r'b)^2\sin(2\beta-2\phi_s) - 2rr'ab\cos(\delta_2-\delta_1) \\ & \times \sin(2\beta+\gamma-\phi_s). \end{aligned} \tag{118}$$

To find out the new contributions due to the fourth generation effect, first we have to evaluate the new Wilson coefficients $C_i^{t'}$. The values of these coefficients at the M_W scale can be obtained from the corresponding contributions from the t quark by replacing the mass of t quark in the Inami-Lim functions [125] by t' mass. These values can then be evolved to the m_b scale using the renormalization group equation [67]

$$\vec{C}(m_b) = U_5(m_b, M_W, \alpha)\vec{C}(M_W), \tag{119}$$

where C is the 10×1 column vector of the Wilson coefficients and U_5 is the five flavor 10×10 evolution matrix. The explicit forms of $\vec{C}(M_W)$ and $U_5(m_b, M_W, \alpha)$ are given in [67]. The values of $\Delta C_{i=1-10}(m_b)$ in the NLO approximation and the coefficients of the dipole operators $C_{7\gamma}^{\rm eff}$ and $C_{8g}^{\rm eff}$ in the LO for different $m_{t'}$ values are presented in Table VI.

For numerical evaluation, we use input parameters as follows. For the form factors and decay constants we use $F_0^{B\to K}(0) = 0.34 \pm 0.05$, $F_0^{B\to\pi}(0) = 0.28 \pm 0.05$, $f_\pi = 0.131$ GeV, $f_K = 0.16$ GeV and for Gegenbauer moments we use $\lambda_B = 350 \pm 150$ MeV [40]. We varied the hard spectator and annihilation phases $\phi_{A,H}$ in the entire range i.e., between $[-\pi, \pi]$, imposing the constraint that the corresponding branching ratios should be within the three sigma experimental range. Also we have included 20% uncertainty in $\Lambda_{\rm QCD}$ i.e., we varied $\Lambda_{\rm QCD} = 225$ MeV from its nominal value in SM3 [40] by ± 45 MeV, which enters in the hard spectator contribution.[8] Since λ_B and $\Lambda_{\rm QCD}$ were previously fixed to 200 MeV and 225 MeV, respectively, to fit the data interpreted in SM3, it may not be unreasonable to assume small changes for SM4. For the CKM matrix elements we use values as given in the Table III. We have also used the range of $\lambda_{t'}$ and ϕ_s as obtained from the fit for different $m_{t'}$.

Using these values we show the allowed regions in the $\Delta A_{CP} - \lambda_{t'}$ plane for different values of $m_{t'}$ in Fig. 11 and we note that an enhancement in ΔA_{CP} upto the current 1σ experimental upper bound ($\approx 17.6\%$) is possible for largeish strong phases, $\phi_{A,H} \sim (-45 \to -90)^\circ$. The correlation plots between mixing induced and direct CP asymmetry parameters in $B^0 \to \pi^0 K^0$ modes are shown in Fig. 12.

TABLE VI. Values of the Wilson coefficients ΔC_i's at different b-mass scale.

$m_{t'}$ (in GeV)	400	600
$\Delta C_3(m_b)$	0.628	1.471
$\Delta C_4(m_b)$	−0.274	−0.578
$\Delta C_5(m_b)$	0.042	0.086
$\Delta C_6(m_b)$	−0.206	−0.362
$\Delta C_7(m_b)$	0.443	1.072
$\Delta C_8(m_b)$	0.168	0.407
$\Delta C_9(m_b)$	−1.926	−4.465
$\Delta C_{10}(m_b)$	0.433	1.005
$\Delta C_{7\gamma}^{\rm eff}(m_b)$	−5.667	−7.239
$\Delta C_{8g}^{\rm eff}(m_b)$	−1.452	−1.728

K. CP violation in $B^0 \to \pi^0\pi^0$ modes

As discussed earlier there exists several hints for the possible existence of new physics in the $b \to s$ sector. So the next obvious question is: Do the $b \to d$ penguin amplitudes also have significant new physics contribution? The present data does not provide any conclusive answer to it. The obvious example is the $B \to \pi\pi$ processes, which receive dominant contribution from $b \to u$ tree and from $b \to d$ penguin diagrams. The present data [60] are presented in Table VII. Thus, it can be seen that the measured value of ${\rm Br}(B^0 \to \pi^0\pi^0)$ is nearly 2 times larger than the corresponding theoretical predictions [40,126]. Also the measured values of direct CP asymmetry parameters $A_{\pi^+\pi^-}$ and $A_{\pi^0\pi^0}$ are higher than the corresponding SM predictions [40]. Thus, the discrepancy between the theoretical and the measured quantities imply that there may also be some new physics effect in the $b \to d$ penguins as speculated in $b \to s$ penguins.

Let us first write down the most general topological amplitudes for $B \to \pi\pi$ modes as

$$\begin{aligned} \sqrt{2}A(B^+ \to \pi^+\pi^0) &= -(T + C + P_{\rm ew}), \\ A(B^0 \to \pi^+\pi^-) &= -(T + P), \\ \sqrt{2}(B^0 \to \pi^0\pi^0) &= -(C - (P - P_{\rm ew})). \end{aligned} \tag{120}$$

[8] The corresponding choices in the scenario S4 of [40] are given by $F_0^{B\to K}(0) = 0.31$, $F_0^{B\to\pi}(0) = 0.25$, $f_\pi = 0.131$ GeV, $f_K = 0.16$ GeV, $\lambda_B = 200$ MeV, $\phi_{A,H} = -55^\circ$, and $\Lambda_{\rm QCD} = 225$ MeV

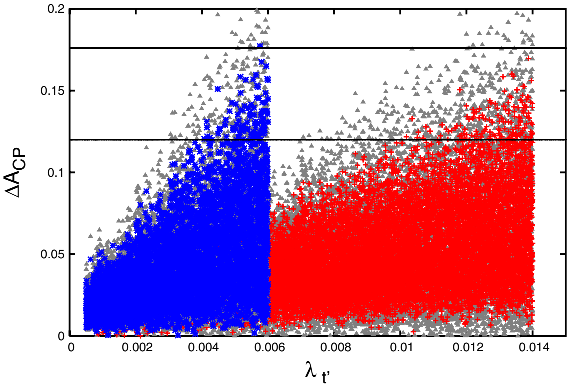

FIG. 11 (color online). The allowed range of the CP asymmetry difference (ΔA_{CP}) in the ($\Delta A_{CP} - \lambda_t'$) plane, where the red and blue regions correspond to $m_{t'} = 400$ and 600 GeV; grey shaded regions correspond to the uncertainties due to hadronic parameters.

From the above relations it can be seen that if there will be additional new contribution to the penguin sector with other amplitudes as expected in SM4 then that may explain $B \to \pi\pi$ observations.

As discussed earlier, due to the presence of the additional generation of quarks the unitarity condition becomes

TABLE VII. Experimental results for $B \to \pi\pi$ processes.

Decay mode	HFAG average
$10^6 \times \mathrm{Br}(B^0 \to \pi^+\pi^-)$	5.16 ± 0.22
$10^6 \times \mathrm{Br}(B^- \to \pi^-\pi^0)$	5.59 ± 0.41
$10^6 \times \mathrm{Br}(B^0 \to \pi^0\pi^0)$	1.55 ± 0.19
$S_{\pi^+\pi^-}$	-0.65 ± 0.07
$A_{\pi^+\pi^-}$	0.38 ± 0.06
$A_{\pi^-\pi^0}$	0.06 ± 0.05
$A_{\pi^0\pi^0}$	$0.43^{+0.25}_{-0.24}$

$\lambda_u + \lambda_c + \lambda_t + \lambda_{t'} = 0$. Thus, including the new contributions one can symbolically represent these amplitudes as

$$\begin{aligned}\mathrm{Amp} &= \lambda_u^d A_u^d + \lambda_c^d A_c^d - \lambda_{t'}^d A_{\mathrm{new}} \\ &= \lambda_u^d A_u^d [1 - r_1 a_1 e^{i(\delta_1^d + \gamma)} - r_1' b_1 e^{i(\delta_2^d + \phi_d)}], \end{aligned} \tag{121}$$

where $b_1 = |\lambda_{t'}^d / \lambda_u^d|$, ϕ_d is the weak phase of $\lambda_t'^d$. $r_1' = |A_{\mathrm{new}}/A_u^d|$, and δ_2^d is the relative strong phases between A_{new} and A_u^d. Thus from the above amplitude one can obtain the CP averaged branching ratio, direct and mixing induced CP asymmetry parameters as

$$\begin{aligned}\mathrm{Br} &= \frac{|p_{\mathrm{c.m}}|\tau_B}{8\pi M_B^2}[\mathcal{R}_1 - 2r_1a_1\cos\delta_1^d\cos\gamma - 2r_1'b_1\cos\delta_2^d\cos(\phi_d+\gamma) + 2r_1r_1'a_1b_1\cos(\delta_2^d - \delta_1^d)\cos\phi_d], \\ A_{\pi\pi} &= \frac{2[r_1a_1\sin\delta_1^d\sin\gamma + r_1'b_1\sin\delta_2^d\sin(\phi_d+\gamma) + r_1r_1'a_1b_1\sin(\delta_1^d - \delta_2^d)\sin\phi_d]}{[\mathcal{R}_1 - 2r_1a_1\cos\delta_1^d\cos\gamma - 2r_1'b_1\cos\delta_2^d\cos(\phi_d+\gamma) + 2r_1r_1'a_1b_1\cos(\delta_2^d - \delta_1^d)\cos\phi_d]}, \\ S_{\pi\pi} &= \frac{X_1}{[\mathcal{R}_1 - 2r_1a_1\cos\delta_1^d\cos\gamma - 2r_1'b_1\cos\delta_2^d\cos(\phi_d+\gamma) + 2r_1r_1'a_1b_1\cos(\delta_2^d - \delta_1^d)\cos\phi_d]},\end{aligned} \tag{122}$$

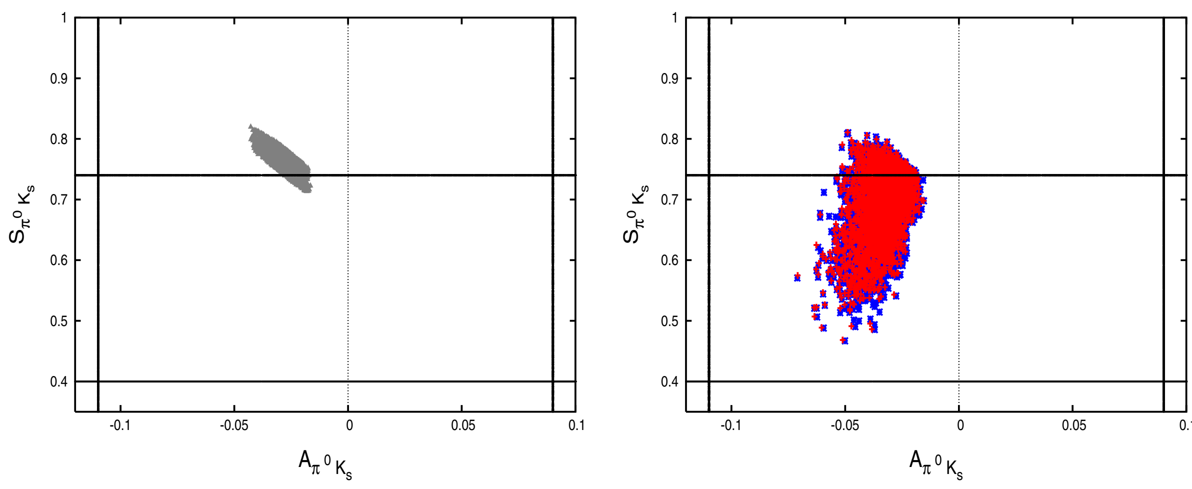

FIG. 12 (color online). Correlation plots between the mixing induced CP asymmetry $S_{\pi^0 K_s}$ and the direct CP asymmetry $A_{\pi^0 K_s}$ in the SM (left panel) and in the fourth generation model (right panel) where the red and blue regions correspond to $m_{t'} = 400$ and 600 GeV. The horizontal and vertical lines represent 1σ experimental allowed ranges.

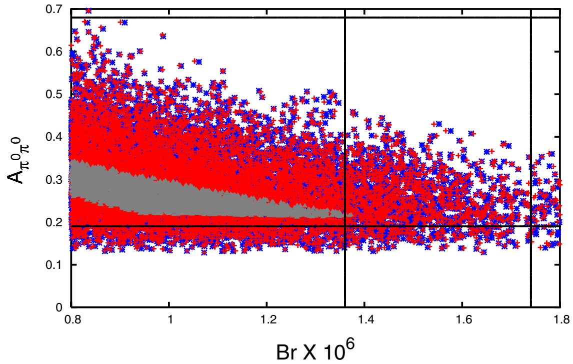

FIG. 13 (color online). The correlation plot between the direct *CP* asymmetry and the *CP*-averaged branching ratio for the $B^0 \to \pi^0\pi^0$ process where the grey region corresponds to the SM result and the red and blue regions correspond to $m_{t'} = 400$ and 600 GeV, respectively. The horizontal and vertical lines represent the 1-σ experimental range of the corresponding observables.

where

$$X_1 = -[\sin(2\beta + 2\gamma) - 2r_1 a_1 \cos\delta_1^d \sin(2\beta + \gamma) + 2r_1' b_1 \cos\delta_2^d \sin(\phi_d - (2\beta + \gamma)) + (r_1 a_1)^2 \sin(2\beta) + (r_1' b_1)^2 \sin(2\phi_d - 2\beta) - 2r_1 r_1' a_1 b_1 \cos(\delta_1^d - \delta_2^d) \sin(\phi_d - 2\beta)]. \quad (123)$$

and $\mathcal{R}_1 = 1 + (r_1 a_1)^2 + (r_1' b_1)^2$. Now varying $\lambda_{t'}^d$ between 0 and 1.5×10^{-4} and ϕ_d between (0–360)° we present the correlation plot between the direct *CP* asymmetry parameter and branching ratio in Fig. 13. From the figure one can see that the observed data could be accommodated in the SM with four generations.

IV. SUMMARY AND OUTLOOK

Standard model with four generations should be considered seriously. We do not have a good understanding of fermion generations. We have already seen three; why not the fourth? Electroweak precision tests do not rule out the existence of a fourth family, though they do require that the mass difference between the t' and the b' be less than about 75 GeV. This degeneracy amounting to $O(10\%)$ for $\approx$ 500 GeV masses does not seem so serious. Of course, the electroweak precision tests suggest then a possible heavy Higgs particle but this actually may be hinting at a very interesting resolution to the hierarchy puzzle. This is because heavier quarks of the 4th generation can play a significant role in dynamical electroweak-symmetry breaking, i.e. a composite Higgs particle.

Another extremely interesting implication of a 4th family is the gigantic improvement over the three generation case in the context of baryogenesis, as, in particular, emphasized by Hou [17].

These two implications of a 4th family are in themselves so interesting, if not profound, that even though at this time the repercussions for dark matter and/or unification are not quite clear, the idea should be given a serious consideration.

Although one of us (A. S.) had gotten already interested and involved in the physics of the 4th generation over 20 years ago, our recent interest was instigated by the fact that this obvious extension of the standard model offers a simple solution to many of the anomalies that have been seen in B, B_s decays. For one thing the predicted value of $\sin 2\beta$ in the SM is coming out to be too high from the one directly measured via the gold-plated ψK_s mode. Besides, the value of $\sin 2\beta$ measured via many of the penguin-dominated modes is systematically coming out to be smaller than the predicted value. Then there is the very large difference in the direct *CP* asymmetry between $K^+\pi^-$ and $K^+\pi^0$ decays of the B^0 and B^+. Finally, there is the fact that both CDF and D0 find that $B_s \to \psi\phi$ decays are exhibiting O(2σ) nonvanishing *CP* asymmetries whereas SM predicts vanishing small asymmetry.

The effect seen in $B_s \to \psi\phi$ at Fermilab is doubly significant. First of all two of the anomalies discussed above that were seen at B-factories taken seriously suggest a nonstandard *CP*-odd phase in $b \to s$ transitions. That then makes it extremely difficult, if not impossible, for new physics not to show up as well in B_s mixing; thus the B-factory anomalies basically imply nonstandard *CP* effects in mixing induced *CP*-asymmetry in $B_s \to \psi\phi$. The second crucial aspect of the *CP* asymmetry in $B_s \to \psi\phi$ is that it is a gold-plated effect; that is, the fact that in the SM *CP* asymmetry in that mode should be vanishingly small is a very clean prediction with no serious hadronic uncertainty. Therefore, it is extremely important that Fermilab gives very high priority to confirming or refuting this effect. In fact very soon the LHCb experiment at CERN should also be able to study this mode and clarify this issue.

In an earlier paper we had focused on studying the *CP* anomalies seen in B, B_s decays in SM4 mentioned above; we found that the SM4 offers a simple explanation for most of the anomalies with the heavy quarks of mass around 400–600 GeV. This paper is a follow up wherein we further explore the implications of SM4 for K and B, B_s decays. By using a host of measurements in K, B, B_s decays such as indirect *CP* violation parameter ϵ_K, $K^+ \to \pi^+\nu\bar{\nu}$, mixing induced *CP* asymmetry in $B \to \psi K_s$, $\mathrm{Br}(B \to X_s\gamma)$, semileptonic decays of B etc. along with oblique parameters and $\mathrm{Br}(Z \to b\bar{b})$, we first constrained the enlarged 4×4 CKM-matrix. We then explored the implications of the SM4 for a variety of processes such as $a_{CP}(B \to X_s\gamma)$, $\mathrm{Br}(B_s \to \mu^+\mu^-)$, $a_{CP}(B \to X_s l^+l^-)$, $A_{\mathrm{SL}}(B_s \to X_s\ell\nu)$, $A_{\mathrm{FB}}(B \to X_s l^+l^-)$, $A_{\mathrm{FB}}(B \to K^* l^+l^-)$, $\mathrm{Br}(B \to X_s\nu\bar{\nu})$, *CP* asymmetries in $B \to \pi^0 K_s$ and in $B \to \pi^0\pi^0$, etc. We identified many processes wherein SM4 predicts significant differences from SM3, e.g. $S(B_s \to \psi\phi)$,

$a_{CP}(B \to X_s \gamma)$, $a_{CP}(B \to X_s l^+ l^-)$, $A_{\rm SL}(B_s \to X_s \ell \nu)$, $\mathrm{Br}(B \to X_s \nu \bar{\nu})$, $\mathrm{Br}(B_s \to \mu^+ \mu^-)$, $\mathrm{Br}(K_L \to \pi^0 \nu \bar{\nu})$, etc.; thus studies therein should especially provide further understanding of the parameter space of SM4.

One of the most interesting aspects of the 4th generation hypothesis is that it is testable relatively easily in the LHC experiments where in fact it has distinctive signatures [17]. In the coming few years not only should we be able to learn about the existence or lack thereof of quarks and leptons of the 4th family, the heavier Higgs that is also favored in the SM4 scenario should be easier to search for in the LHC experiments via the gold-plated mode: $H \to ZZ$. Also the heavy Higgs has interesting implications for flavor-diagonal and flavor-changing final states involving t' and/or b' [127]. Therefore, LHC should shed significant light on the question of SM4 in the next few years.

ACKNOWLEDGMENTS

We want to thank Andrzej Buras, Martin Beneke, Thorsten Feldmann, Tillmann Heidsieck, Alexander Lenz, and Giovanni Punzi for many discussions. S. N. would also like to thank Carlo Giunti for discussion regarding numerical analysis and the theory division of Saha Institute of Nuclear Physics (SINP), in particular, to Gautam Bhattacharyya, for hospitality. The work of A. K. A. is financially supported by NSERC of Canada. The work of A. S. is supported in part by the U.S. DOE Grant No. DE-AC02-98CH10886(BNL). The work of A. G. is supported in part by CSIR and DST, Govt. of India and the work of RM is supported in part by DST, Govt. of India. S. N's work is supported in part by MIUR under Contract No. 2008H8F9RA_002 and by the European Community's Marie-Curie Research Training Network under Contract No. MRTN-CT-2006-035505 Tools and Precision Calculations for Physics Discoveries at Colliders.

Note added in proof.—After our paper was submitted, the D0 experiment at Fermilab [128,129] announced the observation of a CP violating dimuon asymmetry, $A^b_{sl} = -0.009\,57 \pm 0.002\,51 \pm 0.001\,46$, which apparently deviates from the expectation of the standard model, $A^b_{sl}(\mathrm{SM}) = (-2.3^{+0.5}_{-0.6}) \times 10^{-4}$, by about 3.2σ. The measured asymmetry is a linear combination of the asymmetry in B_d and in B_s. Using then the measured asymmetry in B_d from the B factories [130], the D0 Collaboration shows the asymmetry in B_s mixing is $a^s_{sl} = -0.0146 \pm 0.0075$, where the stated error is obtained by adding in quadrature statistical and systematic errors. This measurement differs from the SM prediction of $a^s_{sl}(\mathrm{SM}) = (2.1 \pm 0.6) \times 10^{-5}$ by about 1.9σ. We want to draw attention to the fact that Fig. 3 in our paper shows that a^s_{sl} in SM4 can reach around -0.003 and thus can be a lot bigger than in SM3 but still seems to be somewhat smaller than the central value of the D0 result.

[1] N. Cabibbo, Phys. Rev. Lett. **10**, 531 (1963).
[2] M. Kobayashi and T. Maskawa, Prog. Theor. Phys. **49**, 652 (1973).
[3] E. Lunghi and A. Soni, J. High Energy Phys. 09 (2007) 053.
[4] E. Lunghi and A. Soni, Phys. Lett. B **666**, 162 (2008).
[5] E. Lunghi and A. Soni, J. High Energy Phys. 08 (2009) 051.
[6] A. Lenz and U. Nierste, J. High Energy Phys. 06 (2007) 072.
[7] M. Bona *et al.* (UTfit Collaboration), PMC Phys. A **3**, 6 (2009).
[8] K. Agashe, G. Perez, and A. Soni, Phys. Rev. Lett. **93**, 201804 (2004).
[9] K. Agashe, G. Perez, and A. Soni, Phys. Rev. D **71**, 016002 (2005).
[10] M. Blanke, A. J. Buras, B. Duling, S. Gori, and A. Weiler, J. High Energy Phys. 03 (2009) 001.
[11] M. Blanke, A. J. Buras, B. Duling, K. Gemmler, and S. Gori, J. High Energy Phys. 03 (2009) 108.
[12] S. Casagrande, F. Goertz, U. Haisch, M. Neubert, and T. Pfoh, J. High Energy Phys. 10 (2008) 094.
[13] V. Barger, L. L. Everett, J. Jiang, P. Langacker, T. Liu, and C. E. M. Wagner, J. High Energy Phys. 12 (2009) 048.
[14] W. Altmannshofer, A. J. Buras, S. Gori, P. Paradisi, and D. M. Straub, Nucl. Phys. **B830**, 17 (2010).
[15] A. Soni, A. K. Alok, A. Giri, R. Mohanta, and S. Nandi, Phys. Lett. B **683**, 302 (2010).
[16] A. Soni, arXiv:0907.2057.
[17] W. S. Hou, Chin. J. Phys. (Taipei) **47**, 134 (2009).
[18] For earlier related works see C. Jarlskog and R. Stora, Phys. Lett. B **208**, 268 (1988); F. del Aguila and J. A. Aguilar-Saavedra, Phys. Lett. B **386**, 241 (1996); F. del Aguila and J. A. Aguilar-Saavedra, and G. C. Branco, Nucl. Phys. **B510**, 39 (1998).
[19] See also, R. Fok and G. D. Kribs, Phys. Rev. D **78**, 075023 (2008).
[20] The importance of rare B-decays for searching for the 4th family was emphasized long ago in W.-S. Hou, R. Willey, and A. Soni, Phys. Rev. Lett. **58**, 1608 (1987), see also [21–24].
[21] W.-S. Hou, A. Soni, and H. Steger, Phys. Rev. Lett. **59**, 1521 (1987).
[22] W.-S. Hou, A. Soni, and H. Steger, Phys. Lett. B **192**, 441 (1987).
[23] C. Hamzaoui, A. I. Sanda, and A. Soni, Nucl. Phys. B, Proc. Suppl. **13**, 494 (1990).
[24] G. Eilam, J. L. Hewett, and T. G. Rizzo, Phys. Rev. D **34**, 2773 (1986); Phys. Lett. B **193**, 533 (1987).
[25] J. Carpenter, R. Norton, S. Siegemund-Broka, and A. Soni,

Phys. Rev. Lett. **65**, 153 (1990). In passing, we note that the quark mass needed for dynamical electroweak symmetry breaking in this work, translated to the fourth family quasidegenerate doublet, gives $m_{t'} \sim 500$ GeV and $m_H \approx \sqrt{2} m_{t'} \sim 700$ GeV.

[26] See the *Proceedings of the First International Symposium on The Fourth Family of Quarks and Leptons, Santa Monica, CA*, edited by D. Cline and A. Soni (New York Academy of Sciences, New York, 1987); see also the *Proceedings of the Second International Symposium on The fourth Family of Quarks and Leptons, Santa Monica, CA* edited by D. Cline and A. Soni (New York Academy of Sciences, New York, 1989).

[27] B. Holdom, Phys. Rev. Lett. **57**, 2496 (1986); **58**, 177(E) (1987); W. A. Bardeen, C. T. Hill, and M. Lindner, Phys. Rev. D **41**, 1647 (1990); C. T. Hill, M. A. Luty, and E. A. Paschos, Phys. Rev. D **43**, 3011 (1991); P. Q. Hung and G. Isidori, Phys. Lett. B **402**, 122 (1997).

[28] P. Q. Hung and C. Xiong, arXiv:0911.3892.

[29] M. Hashimoto and V. A. Miransky, Phys. Rev. D **81**, 055014 (2010).

[30] J. Erler and P. Langacker, Acta Phys. Pol. B **39**, 2595 (2008).

[31] V. A. Novikov, L. B. Okun, A. N. Rozanov, and M. I. Vysotsky, Phys. Lett. B **529**, 111 (2002).

[32] V. A. Novikov, L. B. Okun, A. N. Rozanov, and M. I. Vysotsky, Pis'ma Zh. Eksp. Teor. Fiz. **76**, 158 (2002) [JETP Lett. **76**, 127 (2002)].

[33] G. D. Kribs, T. Plehn, M. Spannowsky, and T. M. P. Tait, Phys. Rev. D **76**, 075016 (2007).

[34] M. S. Chanowitz, Phys. Rev. D **79**, 113008 (2009).

[35] J. Erler and P. Langacker, arXiv:1003.3211.

[36] D. E. Groom *et al.* (Particle Data Group), Eur. Phys. J. C **15**, 1 (2000); M. Maltoni *et al.*, Phys. Lett. B **476**, 107 (2000).

[37] See, e.g. G. E. Volovik, Pis'ma Zh. Eksp. Teor. Fiz. **78**, 1203 (2003) [JETP Lett. **78**, 691 (2003)].

[38] B. Kayser, arXiv:0804.1497.

[39] M. Beneke, G. Buchalla, M. Neubert, and C. T. Sachrajda, Nucl. Phys. **B606**, 245 (2001).

[40] M. Beneke and M. Neubert, Nucl. Phys. **B675**, 333 (2003).

[41] A. Hovhannisyan, W. S. Hou, and N. Mahajan, Phys. Rev. D **77**, 014016 (2008).

[42] A. Arhrib and W. S. Hou, Eur. Phys. J. C **27**, 555 (2003).

[43] W. S. Hou, M. Nagashima, and A. Soddu, Phys. Rev. D **72**, 115007 (2005).

[44] W. S. Hou, M. Nagashima, and A. Soddu, Phys. Rev. Lett. **95**, 141601 (2005).

[45] A. Arhrib and W. S. Hou, J. High Energy Phys. 07 (2006) 009.

[46] W. S. Hou, M. Nagashima, G. Raz, and A. Soddu, J. High Energy Phys. 09 (2006) 012.

[47] W. S. Hou, H. n. Li, S. Mishima, and M. Nagashima, Phys. Rev. Lett. **98**, 131801 (2007).

[48] M. Bobrowski, A. Lenz, J. Riedl, and J. Rohrwild, Phys. Rev. D **79**, 113006 (2009); G. Eilam, B. Melic, and J. Trampetic, Phys. Rev. D **80**, 116003 (2009).

[49] W. S. Hou and C. Y. Ma, have recently updated their analysis; see the talk by C. Y. Ma at the *Second Workshop on Beyond the Three Generation Standard Model* (The National Taiwan University, Taipei, Taiwan, 2010).

[50] D. J. Antonio *et al.* (RBC Collaboration and UKQCD Collaboration), Phys. Rev. Lett. **100**, 032001 (2008).

[51] D. Becirevic, in *Proceedings of 2nd Workshop on the CKM Unitarity Triangle, Durham, England, 2003* [hep-ph/0310072]; N. Tantalo, arXiv:hep-ph/0703241; E. Gamiz, C. T. H. Davies, G. P. Lepage, J. Shigemitsu, and M. Wingate, Proc. Sci., LAT2007 (2007) 349.

[52] H. G. Evans (CDF Collaboration and D0 Collaboration), Frascati Phys. Ser. **44**, 421 (2007).

[53] S. Herrlich and U. Nierste, Nucl. Phys. **B419**, 292 (1994).

[54] A. J. Buras, M. Jamin, and P. H. Weisz, Nucl. Phys. **B347**, 491 (1990).

[55] S. Herrlich and U. Nierste, Phys. Rev. D **52**, 6505 (1995).

[56] M. E. Peskin and T. Takeuchi, Phys. Rev. D **46**, 381 (1992).

[57] P. Q. Hung and M. Sher, Phys. Rev. D **77**, 037302 (2008).

[58] V. A. Novikov, A. N. Rozanov, and M. I. Vysotsky, Phys. At. Nucl. **73**, 636 (2010).

[59] J. Bernabeu, A. Pich, and A. Santamaria, Nucl. Phys. **B363**, 326 (1991).

[60] E. Barberio *et al.* (Heavy Flavor Averaging Group), arXiv:0808.1297.

[61] M. Misiak and M. Steinhauser, Nucl. Phys. **B764**, 62 (2007).

[62] M. Misiak *et al.*, Phys. Rev. Lett. **98**, 022002 (2007); See also, T. Becher and M. Neubert, Phys. Rev. Lett. **98**, 022003 (2007).

[63] A. J. Buras and M. Munz, Phys. Rev. D **52**, 186 (1995).

[64] A. J. Buras and R. Fleischer, Adv. Ser. Dir. High Energy Phys. **15**, 65 (1998); arXiv:hep-ph/9704376.

[65] Y. Nir, Phys. Lett. B **221**, 184 (1989).

[66] T. Hattori, T. Hasuike, and S. Wakaizumi, Phys. Rev. D **60**, 113008 (1999).

[67] G. Buchalla, A. J. Buras, and M. E. Lautenbacher, Rev. Mod. Phys. **68**, 1125 (1996); arXiv:hep-ph/9512380.

[68] A. J. Buras and D. Guadagnoli, Phys. Rev. D **78**, 033005 (2008); arXiv:0805.3887.

[69] C. Aubin, J. Laiho, and R. S. Van de Water, Phys. Rev. D **81**, 014507 (2010).

[70] See also C. Kelly (RBC-UKQCD Collaborations), in Lattice 2009 Symposium, Beijing, China (unpublished).

[71] G. Buchalla and A. J. Buras, Nucl. Phys. **B412**, 106 (1994); arXiv:hep-ph/9308272.

[72] A. J. Buras, B. Duling, T. Feldmann, T. Heidsieck, C. Promberger, and S. Recksiegel, arXiv:1002.2126.

[73] A. L. Kagan and M. Neubert, Phys. Rev. D **58**, 094012 (1998); arXiv:hep-ph/9803368.

[74] K. Kiers, A. Soni, and G. H. Wu, Phys. Rev. D **62**, 116004 (2000); arXiv:hep-ph/0006280.

[75] J. M. Soares, Nucl. Phys. **B367**, 575 (1991).

[76] T. Hurth, E. Lunghi, and W. Porod, Nucl. Phys. **B704**, 56 (2005); arXiv:hep-ph/0312260.

[77] T. E. Browder, T. Gershon, D. Pirjol, A. Soni, and J. Zupan, Rev. Mod. Phys. **81**, 1887 (2009).

[78] T. Aaltonen *et al.* (CDF Collaboration), Phys. Rev. Lett. **100**, 161802 (2008); arXiv:0712.2397; V. M. Abazov *et al.* (D0 Collaboration), Phys. Rev. Lett. **101**, 241801 (2008).

[79] E. H. Thorndike, Annu. Rev. Nucl. Part. Sci. **35**, 195 (1985); J. S. Hagelin and M. B. Wise, Nucl. Phys. **B189**, 87 (1981); J. S. Hagelin, Nucl. Phys. **B193**, 123 (1981);

A. J. Buras, W. Slominski, and H. Steger, Nucl. Phys. **B245**, 369 (1984); R. N. Cahn and M. P. Worah, Phys. Rev. D **60**, 076006 (1999).
[80] K. Anikeev *et al.*, arXiv:hep-ph/0201071.
[81] S. Laplace, Z. Ligeti, Y. Nir, and G. Perez, Phys. Rev. D **65**, 094040 (2002).
[82] V. M. Abazov *et al.* (D0 Collaboration), Phys. Rev. Lett. **98**, 151801 (2007).
[83] CDF Collaboration, CDF Report No. 9015, 2007, http://www.cdf.fnal.gov.
[84] Heavy Flavour Averaging Group (HFAG), http://www.slac.stanford.edu/xorg/hfag/.
[85] E. Franco, M. Lusignoli, and A. Pugliese, Nucl. Phys. **B194**, 403 (1982); L. L. Chau, Phys. Rep. **95**, 1 (1983); M. B. Voloshin, N. G. Uraltsev, V. A. Khoze, and M. A. Shifman, Sov. J. Nucl. Phys. **46**, 112 (1987); A. Datta, E. A. Paschos, and U. Türke, Phys. Lett. B **196**, 382 (1987); A. Datta, E. A. Paschos, and Y. L. Wu, Nucl. Phys. **B311**, 35 (1988).
[86] M. Beneke, G. Buchalla, and I. Dunietz, Phys. Rev. D **54**, 4419 (1996).
[87] M. Beneke, G. Buchalla, C. Greub, A. Lenz, and U. Nierste, Phys. Lett. B **459**, 631 (1999).
[88] M. Ciuchini, E. Franco, V. Lubicz, F. Mescia, and C. Tarantino, J. High Energy Phys. 08 (2003) 031.
[89] M. Beneke, G. Buchalla, A. Lenz, and U. Nierste, Phys. Lett. B **576**, 173 (2003).
[90] T. Gershon and A. Soni, J. Phys. G **34**, 479 (2007).
[91] D. S. Du and M. Z. Yang, Phys. Rev. D **54**, 882 (1996).
[92] A. Ali and G. Hiller, Eur. Phys. J. C **8**, 619 (1999).
[93] A. K. Alok, A. Dighe, and S. Ray, Phys. Rev. D **79**, 034017 (2009).
[94] B. Aubert *et al.* (*BABAR* Collaboration), Phys. Rev. Lett. **93**, 081802 (2004).
[95] M. Iwasaki *et al.* (Belle Collaboration), Phys. Rev. D **72**, 092005 (2005).
[96] A. Ghinculov, T. Hurth, G. Isidori, and Y. P. Yao, Eur. Phys. J. C **33**, s288 (2004); arXiv:hep-ph/0310187.
[97] A. Ali, E. Lunghi, C. Greub, and G. Hiller, Phys. Rev. D **66**, 034002 (2002); arXiv:hep-ph/0112300.
[98] A. Ali, arXiv:hep-ph/0210183.
[99] A. Ali, T. Mannel, and T. Morozumi, Phys. Lett. B **273**, 505 (1991).
[100] T. Huber, T. Hurth, and E. Lunghi, Nucl. Phys. **B802**, 40 (2008).
[101] B. Aubert *et al.* (*BABAR* Collaboration), Phys. Rev. Lett. **91**, 221802 (2003); arXiv:hep-ex/0308042.
[102] B. Aubert *et al.* (*BABAR* Collaboration), Phys. Rev. D **73**, 092001 (2006); arXiv:hep-ex/0604007.
[103] A. Ishikawa *et al.* (Belle Collaboration), Phys. Rev. Lett. **91**, 261601 (2003); arXiv:hep-ex/0308044.
[104] E. Lunghi, arXiv:hep-ph/0210379.
[105] A. Ali, P. Ball, L. T. Handoko, and G. Hiller, Phys. Rev. D **61**, 074024 (2000); arXiv:hep-ph/9910221.
[106] A. J. Buras, Phys. Lett. B **566**, 115 (2003); M. Blanke, A. J. Buras, D. Guadagnoli, and C. Tarantino, J. High Energy Phys. 10 (2006) 003.
[107] Y. Grossman, Z. Ligeti, and E. Nardi, Phys. Rev. D **55**, 2768 (1997).
[108] M. Lenzi, arXiv:0710.5056.
[109] M. Smizanska (ATLAS Collaboration and CMS Collaboration), arXiv:0810.3618.
[110] E. Gamiz, C. T. H. Davies, G. P. Lepage, J. Shigemitsu, and M. Wingate (HPQCD Collaboration), Phys. Rev. D **80**, 014503 (2009).
[111] Y. Grossman, Z. Ligeti, and E. Nardi, Nucl. Phys. **B465**, 369 (1996); **480**, 753(E) (1996); arXiv:hep-ph/9510378.
[112] C. Bobeth, M. Bona, A. J. Buras, T. Ewerth, M. Pierini, L. Silvestrini, and A. Weiler, Nucl. Phys. **B726**, 252 (2005); arXiv:hep-ph/0505110.
[113] R. Barate *et al.* (ALEPH Collaboration), Eur. Phys. J. C **19**, 213 (2001); arXiv:hep-ex/0010022.
[114] A. J. Buras, M. Gorbahn, U. Haisch, and U. Nierste, Phys. Rev. Lett. **95**, 261805 (2005); arXiv:hep-ph/0508165; A. J. Buras, M. Gorbahn, U. Haisch, and U. Nierste, J. High Energy Phys. 11 (2006) 002; J. Brod and M. Gorbahn, Phys. Rev. D **78**, 034006 (2008); arXiv:0805.4119.
[115] Y. Grossman and M. P. Worah, Phys. Lett. B **395**, 241 (1997); arXiv:hep-ph/9612269; Y. Grossman, G. Isidori, and M. P. Worah, Phys. Rev. D **58**, 057504 (1998).
[116] D. London and A. Soni, Phys. Lett. B **407**, 61 (1997).
[117] M. Beneke, Phys. Lett. B **620**, 143 (2005).
[118] H. Y. Cheng, C. K. Chua, and A. Soni, Phys. Rev. D **71**, 014030 (2005); H. Y. Cheng, C. K. Chua, and A. Soni, Phys. Rev. D **72**, 014006 (2005).
[119] G. Buchalla, G. Hiller, Y. Nir, and G. Raz, J. High Energy Phys. 09 (2005) 074.
[120] R. Fleischer, S. Jager, D. Pirjol, and J. Zupan, Phys. Rev. D **78**, 111501 (2008).
[121] M. Gronau and J. L. Rosner, Phys. Lett. B **666**, 467 (2008).
[122] S. Baek, C. W. Chiang, M. Gronau, D. London, and J. L. Rosner, Phys. Lett. B **678**, 97 (2009).
[123] I. Adachi *et al.* (Belle Collaboration), Phys. Rev. D **81**, 011101 (2010).
[124] B. Aubert *et al.* (*BABAR* Collaboration), Phys. Rev. D **79**, 052003 (2009).
[125] T. Inami and C. S. Lim, Prog. Theor. Phys. **65**, 297 (1981); **65**, 1772 (1981).
[126] H. n. Li, S. Mishima, and A. I. Sanda, Phys. Rev. D **72**, 114005 (2005); H. n. Li and S. Mishima, Phys. Rev. D **73**, 114014 (2006).
[127] S. Bar-Shalom, G. Eilam, and A. Soni, Phys. Lett. B **688**, 195 (2010).
[128] V. M. Abazov *et al.* (D0 Collaboration), arXiv:1005.2757.
[129] We thank Guennadi Borissov and Daria Zieminska for helpful discussions related to the D0 observations.
[130] E. Barberio *et al.* (Heavy Flavor Averaging Group), arXiv:0808.1297.